Titre: Title:	A simple model of internal erosion in embankment dams
Auteur: Author:	Quynh Trang Mach
Date:	2009
Type:	Mémoire ou thèse / Dissertation or Thesis
Référence: Citation:	Mach, Q. T. (2009). A simple model of internal erosion in embankment dams [Master's thesis, École Polytechnique de Montréal]. PolyPublie. https://publications.polymtl.ca/8476/

UNIVERSITÉ DE MONTRÉAL

A SIMPLE MODEL OF INTERNAL EROSION IN EMBANKMENT DAMS

QUYNH TRANG MACH
DÉPARTEMENT DES GÉNIES CIVIL GÉOLOGIQUE ET DES MINES
ÉCOLE POLYTECHNIQUE DE MONTRÉAL

MÉMOIRE PRÉSENTÉ EN VUE DE L'OBTENTION
DU DIPLÔME DE MAÎTRISE ÈS SCIENCES APPLIQUÉES
(GÉNIE CIVIL)
AOUT 2009

Your file Votre référence
ISBN: 978-0-494-57257-3
Our file Notre référence
ISBN: 978-0-494-57257-3

UNIVERSITÉ DE MONTRÉAL

ÉCOLE POLYTECHNIQUE DE MONTRÉAL

Ce mémoire intitulé:

A SIMPLE MODEL OF INTERNAL EROSION IN EMBANKMENT DAMS

présenté par: MACH Quynh Trang

en vue de l'obtention du diplôme de: Maîtrise ès sciences appliquées

a été dûment accepté par le jury d'examen constitué de:

M. ROBILLARD Luc, Ph.D., président

M. KAHAWITA René, Ph.D., membre et directeur de recherche

M. NGUYEN T. Hung, Ph.D., membre et codirecteur de recherche

M. LECLERC Guy, PhD., membre

ACKNOWLEDGEMENTS

First of all, I would like to express my greatest appreciation and gratitude to Professor René Kahawita for his guidance and encouragement during all phases of my graduate study in the Department of Civil Geological and Mining Engineering. His insight into the fundamental aspect of the physical phenomena and his ingenuity in solving practical problems have greatly helped me in achieving this thesis. He gave me a true interest in doing scientific research. It was a really great pleasure to work under his wise guidance.

I should thank Professor The Hung Nguyen for introducing me to the domain of fluid flow in porous media and for his ongoing advice during the course of my studies.

I would like to thank Professors Guy Leclerc and Luc Robillard for having kindly accepted to evaluate my work.

I would also like to thank my family, my friends and colleagues for their unconditional support and encouragement.

Finally, I would like to acknowledge the National Science and Engineering Research Council (NSERC) of Canada for the financial support during my study at École Polytechnique.

RÉSUMÉ

Les digues et barrages construits en terre et en pierre sont des ouvrages hydrauliques les plus communs pour l'approvisionnement de l'eau, l'irrigation, la navigation, la production d'énergie, etc. La rupture de ces ouvrages peut causer des dommages catastrophiques tant humains qu'économiques. Les deux causes principales de ces ruptures sont dues au débordement continu de l'eau au-dessus des digues ou à l'érosion interne incontrôlée qui entrainerait le phénomène de renard. Ce mémoire est consacré à ce dernier phénomène, et en particulier, à construire un modèle mathématique basé sur les mécanismes physiques du phénomène.

L'érosion interne est un phénomène qui pourrait se produire lorsque le gradient de pression dans un barrage dépasse une certaine valeur critique de telle sorte que les particules fines soient arrachées de la structure du sol et entrainées par l'écoulement de l'eau. La durée de ce processus, du début de l'érosion jusqu'à la rupture du barrage, peut varier de quelques heures à plusieurs années. Afin de prédire l'effondrement d'un barrage, il est nécessaire de comprendre ce processus avant de déterminer sa stabilité. C'est un problème très complexe et il est indispensable de comprendre les mécanismes fondamentaux associés aux différentes échelles de temps afin de prédire son évolution et d'analyser la stabilité de la structure du barrage.

Une analyse des récents travaux théoriques et expérimentaux sur l'érosion interne montre qu'il n'est pas encore possible de prédire ce qui se passe dans un barrage lorsque le gradient de pression augmente. Dans une séries d'études expérimentales, Bendahmane et collaborateurs ont montré que le taux d'érosion devrait être proportionnel à $q(1-\phi)/\phi$, q et ϕ étant la vitesse de filtration et la porosité du milieu. Dans une autre série d'expériences, Vardoulakis et collaborateurs ont trouvé que le taux d'érosion devrait varier comme $q(1-\phi)C$, C étant la concentration des particules qui sont détachées de la structure du sol et sont entraînées dans l'écoulement de l'eau. Selon la loi d'érosion de

Bendahmane, la porosité devrait être spatialement uniforme durant tout le processus d'érosion, ce qui serait vrai seulement dans le processus de suffusion. Par contre, d'après la loi d'érosion de Vardoulakis, la porosité devrait augmenter dans la direction de l'écoulement. C'est le phénomène de renard (backward erosion) où un 'tunnel' est creusé de l'aval vers l'amont de l'écoulement. Afin d'unifier ces deux situations, il est essentiel de trouver une équation qui relie le taux d'érosion aux principaux paramètres caractéristiques du problème. Notre approche consiste à construire un modèle qui comprend deux mécanismes qui puissent entrer simultanément en jeu dans ce processus, soient les interactions fluide-particule et les interactions particule-particule. Nous considérerons ainsi tout d'abord les effets des forces de cisaillement exercées par l'écoulement de l'eau sur les particules fixes du sol. Nous considérons ensuite les effets des particules détachées qui se déplacent avec l'eau. Au cours de leurs déplacements, ces particules peuvent entrer en collision avec les particules fixes et par conséquent les arracher de la structure du sol. En combinant les effets des interactions fluide-particule avec les effets des interactions particule-particule, nous arrivons alors à un modèle mathématique qui peut décrire aussi bien le phénomène de suffusion que le phénomène de renard. En fait, les résultats obtenus précédemment par Bendahmane et Vardoulakis peuvent être retrouvés comme des cas limites de notre modèle. Les résultats obtenus montrent que ce modèle pourrait simuler l'évolution du phénomène d'érosion interne sous différentes conditions, du processus de suffusion jusqu'au processus de renard. Ces résultats indiquent ainsi une nouvelle direction de recherche qui permettrait d'arriver à un modèle plus général pour un plus grand éventail de problèmes. Il faut noter que le modèle proposé ne peut pas prédire la rupture des barrages, mais nous aide plutôt à mieux comprendre un phénomène très complexe.

ABSTRACT

Embankment dams are water barriers constructed of earth and rock. They are the most common type of dams used to impound water for a variety of purposes such as for water supply, irrigation, navigation and power generation. The failure of an embankment dam will generally lead to catastrophic consequences such as the loss of life as well as economic losses. The two principal causes of failure in an embankment dam is due to prolonged overtopping at the crest or by uncontrolled internal erosion leading to a phenomenon known as 'piping'. This thesis is an attempt to model the second failure mechanism, i.e. internal erosion which if unchecked may lead to destruction. In particular, an attempt has been made to develop a numerical model based on a simplified representation of the physically based processes that underlies the phenomenon.

Internal erosion is a process by which soil particles from the interior of the dam are detached and carried downstream by the seepage (water) flow when the pressure gradient across the dam exceeds a certain critical value. The duration of the erosion process, from the inception of erosion to the complete breakdown of the dam may vary from a few hours to many years. Clearly, the problem is not trivial and to predict the likelihood of failure requires an understanding of the intrinsic processes together with their associated time scales. It may then be possible to make an assessment of the stability of the structure for purposes of dam safety analyses.

An analysis of the most recent theoretical and experimental work on internal erosion reveals that what may happen in an embankment dam as the pressure gradient increases is still largely unpredictable. Based on a series of experimental studies, Bendahmane and his co-workers (2005) concluded that the erosion rate of fine particles in a porous matrix should be directly proportional to $q(1-\phi)/\phi$, where q is the filtration velocity and ϕ is the porosity of the medium. In an independent series of experimental tests, Vardoulakis and co-workers (1996) found that the erosion rate should vary as $q(1-\phi)C$ where C is the concentration of eroded particles that move with the water. According to the erosion

rate found by Bendahmane et al. (2005) the porosity of the medium would be expected to remain spatially uniform during the whole process. This may be true only during the so-called suffusion process. From the erosion rate found by Vardoulakis et al. (1996) however, the porosity of the medium would be expected to increase in the downstream direction. This non-uniform erosion may occur in the so-called backward erosion process where a 'tunnel' could gradually make its way upstream, from the (downstream) exit point of the water into the interior of the dam. To unify these two situations, the key question is to find a model equation for the rate of erosion in terms of the most significant parameters of the problem. The strategy adopted in this work is to construct a model of internal erosion by considering the fluid-particle and particle-particle interactions as two simultaneous eroding mechanisms. Initially, the shear force effects of the interstitial flow on the erosion rate of the soil structure are considered. Subsequently, it is postulated that these suspended particles detached from the soil structure and transported by the flow may have the effect of successfully dislodging (by collision) additional particles bound to the exposed soil structure. By combining these two mechanisms of erosion, namely the fluid-particle interactions and the particle-particle interactions, it has been possible to construct a mathematical model that appears to describe both the suffusion as well as the backward erosion phenomena. In fact, the results obtained previously by Bendahmane and Vardoulakis may be recovered as two limiting cases of the present model. The results obtained with this model indicate that it may be used to simulate the evolution of internal erosion in a variety of situations, from the slow suffusion process to the strong backward erosion stage, leading to the piping failure. These results also provide guidance towards searching for a more general model to predict the erosion process in a greater class of problems. As the present model stands, it can in no way be considered a predictive tool but rather as an aid to understanding what is obviously a complex process.

CONDENSÉ EN FRANÇAIS

Les barrages et digues en terre sont des ouvrages hydrauliques les plus communs pour l'approvisionnement de l'eau, l'irrigation, et la production d'énergie. La rupture de ces ouvrages est généralement due au débordement continu de l'eau au-dessus des barrages ou à l'érosion interne incontrôlée des particules constituantes. En fait, les statistiques de l'ICOLD (International Committee on Large Dams) ont démontré que la rupture des barrages en terre est plus fréquente que celle d'autres types de barrages, et que l'érosion interne en est le plus souvent la cause. Par conséquent, l'érosion interne doit être considérée comme un problème majeur dans la rupture des barrages en terre.

L'érosion interne est due à l'arrachement et la migration des particules constituantes sous l'action d'un écoulement à travers le barrage, ce qui provoque une modification de la granulométrie du sol, et le rend plus poreux et moins stable. La durée de ce processus, du début de l'érosion jusqu'à la rupture du barrage, peut varier de quelques heures à plusieurs années. Afin de prédire l'effondrement d'un barrage, il est indispensable de comprendre les mécanismes fondamentaux associés aux différentes échelles de temps afin de prédire son évolution et d'analyser la stabilité de la structure du barrage.

L'érosion des particules peut se produire sous forme de suffusion et d'érosion régressive (backward erosion). La suffusion est le phénomène d'érosion de grains de petite taille lorsque la vitesse locale dépasse une certaine limite. Elle se développe au sein d'un barrage lorsque la granulométrie n'assure pas l'autofiltration. L'érosion régressive (ou phénomène de renard) est l'arrachement des particules progressant de l'aval vers l'amont de l'écoulement, jusqu'à la formation d'un conduit continu.

Dans le cadre de ce mémoire, notre objectif est de construire un modèle mathématique permettant de simuler l'évolution du processus d'érosion provoquée par ces deux phénomènes, soit indépendamment, soit simultanément.

Ce mémoire est composé de cinq chapitres.

Dans le premier chapitre, nous présentons un aperçu général du problème d'érosion interne des barrages. On y trouvera une description des étapes principales du processus

d'érosion interne, notamment l'initiation, la continuation, et la progression de l'érosion vers la rupture, ainsi que les critères et le temps de développement de ces étapes.

Le deuxième chapitre est consacré à une revue des travaux existants qui forment la base pour le développement de notre modèle. On y trouvera les résultats de plusieurs études portant spécifiquement sur le phénomène de suffusion et d'érosion régressive, notamment celles de Khilar et Fogler (1998), Wan et Fell (2004), Bonelli et al. (2007), Sterpi (2003), Bendahmane (2005), et Vardoulakis et al (1996). L'objectif général de ces travaux est de mieux comprendre les caractéristiques du processus d'érosion interne dans différents types de matériaux et sous différentes contraintes hydrauliques, et d'essayer de déterminer le taux d'érosion en fonction des paramètres de contrôle du problème. Les trois premiers auteurs (Khilar et Fogler, Wan et Fell, Bonelli et al) ont proposé une équation constitutive de la forme

$$r_{er} = k_{er}\left(\tau_w - \tau_c\right)$$

où r_{er} est le taux d'érosion par unité de surface érosive, τ_w est le taux de cisaillement exercé par le fluide sur les particules solides, τ_c est le taux de cisaillement critique, et k_{er} est le coefficient d'érosion. La différence entre ces études réside dans la détermination de ce dernier coefficient et du taux de cisaillement critique τ_c, deux paramètres qui peuvent varier largement d'un modèle à l'autre.

Dans une étude du problème d'érosion du sous-sol de la région de Milan (Italie), Sterpi a réalisé une expérience lui permettant d'arriver à l'expression empirique suivante pour le taux d'érosion des particules fines :

$$S = \rho_0 \cdot \left(-\frac{b}{t_0}\right) \cdot \left(\frac{t}{t_0}\right)^{b-1} \cdot \frac{i^c}{a} \cdot \exp\left[-\left(\frac{t}{t_0}\right)^b \cdot \frac{i^c}{a}\right]$$

où S est le taux d'érosion par unité de volume de sol, ρ_0 est la densité des particules fines, t_0 = 1 heure, a, b, c sont des constantes (empiriques) adimensionnelles, t est le temps, and i est le gradient hydraulique. Dans cette expérience, la variation de la perméabilité étant très faible et le gradient hydraulique étant constant, le taux d'érosion

varie ainsi seulement avec le temps, et la porosité demeure spatialement uniforme. Le processus d'érosion dans cette expérience correspond donc au phénomène de suffusion. Le travail de Bendahmane est une étude expérimentale du phénomène de suffusion suivi d'une modélisation numérique basée sur une équation constitutive pour le taux d'érosion de la forme

$$S = \rho_s \lambda \frac{(1-\phi)}{\phi} q$$

où S est le taux d'érosion par unité de volume du milieu érosif, ρ_s est la densité des particules solides, λ est le coefficient d'érosion, ϕ est la porosité, q est le débit par unité de surface. Ce modèle a permis de reproduire l'allure générale de l'évolution et les ordres de grandeur de masse érodée obtenue expérimentalement. La différence remarquable entre l'expérience et la théorie se situe au niveau de la perméabilité du milieu : Les expériences montrent qu'elle subit une très forte diminution (d'un facteur de 10) tandis que le modèle prévoit une perméabilité constante dans le temps.

En relation avec la production de sable dans les puits d'exploitation du pétrole, Vadoulakis et al. (1996) ont présenté un modèle mathématique du phénomène d'érosion basée sur une équation constitutive pour le taux d'érosion de la forme

$$S = \rho_s \lambda (1-\phi) C q$$

où C est la concentration volumique des particules érodées. La différence essentielle entre cette équation et celle de Bendahmane est la présence de la concentration C. Les résultats obtenus par Vadoulakis et al (1996) ont montré que la porosité augmente avec le temps comme on peut prévoir avec le modèle de Bendahmane. Mais contrairement à ce dernier, elle augmente également dans la direction de l'écoulement, ce qui correspond à une érosion régressive, de l'aval vers l'amont. Les expériences et les modèles

mathématiques de Bendahmane (2005) et de Vadoulakis (1996) correspondent ainsi aux deux phénomènes distincts, soit la suffusion et l'érosion régressive.

Le chapitre 3 constitue l'essentiel de notre travail. Nous y proposons un modèle mathématique permettant de simuler à la fois le phénomène de suffusion et le phénomène d'érosion régressive dans un processus d'érosion interne, en considérant deux mécanismes qui peuvent entrer simultanément en jeu dans ce processus, soient les interactions fluide-particule et les interactions particule-particule.

Notre modèle consiste à considérer le barrage comme un milieu poreux constitué de deux types de particules solides, les 'grosses' et les 'fines'. L'écoulement de l'eau à travers le barrage est régi par la loi de Darcy.

Le transport des particules érodées qui sont entrainées dans l'écoulement de l'eau est régi par la loi de conservation de la masse, soit

$$\frac{\partial(C\phi)}{\partial t} + q\frac{\partial C}{\partial x} = S$$

où le taux d'érosion S est relié à la loi de conservation des particules solides fixes, soit

$$\frac{\partial \phi}{\partial t} = \frac{S}{\rho_s}$$

La difficulté principale du problème réside dans la détermination d'une équation constitutive pour le taux d'érosion S en fonction des paramètres caractéristiques tels que le gradient de pression, la porosité, la concentration des particules fixes et celle des particules érodées. Nous considérons d'abord les effets de la force de cisaillement exercée par l'écoulement de l'eau sur les particules fixes du sol. C'est cette force qui est responsable de l'initiation du processus d'érosion. En se basant sur la formule de Stokes pour la force de traînée sur une sphère, nous déduisons la formule suivante pour le taux d'érosion due à l'interaction fluide-particule :

$$S_D = \frac{6a\lambda^* \mu}{\pi d^2}(\phi_{\max} - \phi)\frac{q}{\phi}$$

D'un autre côté, les particules érodées peuvent, durant leur déplacement au sein du milieu poreux, entrer en collision avec les particules fixes et les arracher de la structure solide. Le taux d'érosion due à ces interactions particule-particule doit être proportionnel à la vitesse ainsi qu'aux nombres des particules mobiles et des particules fixes. Nous pouvons alors exprimer ce taux sous la forme

$$S_M = \frac{6b\rho_s}{\pi d^3}(\phi_{\max} - \phi)Cq$$

En combinant ces deux interactions, fluide-particule et particule-particule, nous arrivons à l'équation constitutive suivante pour le taux d'érosion :

$$S = \rho_s(\phi_{\max} - \phi)q\left[\frac{A}{\phi} + BC\right]$$

où A et B sont deux paramètres à déterminer empiriquement.

Notre modèle mathématique du phénomène d'érosion interne est donc décrit par le système d'équations suivantes :

$$\frac{\partial \phi}{\partial t} = (\phi_{\max} - \phi)q\left[\frac{A}{\phi} + BC\right]$$

$$\frac{\partial (C\phi)}{\partial t} + q\frac{\partial C}{\partial x} = \frac{\partial \phi}{\partial t}$$

avec le débit q donné par l'équation de Darcy

$$q = -(k/\bar{\mu})(dP/dx + \rho g dz/dx)$$

où k est la perméabilité déterminée par la formule

$$k = k_0 \frac{\phi^3}{\left[(1-\phi) + \frac{\sqrt{2k_o}}{R_o} \right]^2}$$

qui est la formule de Carman-Kozeny modifiée pour $\phi < 1$, et se réduit à celle d'un tuyau vide lorsque $\phi = 1$.

Les résultats obtenus en résolvant numériquement ce système d'équations par la méthode des différences finies sont présentés au chapitre 4.

Nous considérons d'abord le cas où seule la suffusion peut se produire à travers le milieu, c.-à-d. lorsque le détachement des particules solides est dû seulement à la force de traînée de l'écoulement fluide.

Nous retrouvons les même résultats que ceux de Bendahmane en posant $B = 0$ et en utilisant les même valeurs pour le paramètre A. Nous procédons ensuite à étudier les effets du coefficient d'érosion A en résolvant le problème pour $A = 0.5$, 1 et 2, respectivement. Les résultats obtenus montrent que la porosité et le débit augmentent toutes deux continuellement avec le temps, mais restent spatialement uniformes, ce qui est dû au fait que l'écoulement est supposé unidimensionnel et que le taux d'érosion dépend seulement de la porosité et du débit. La concentration des particules érodées augmente cependant dans la direction de l'écoulement. Elle atteint une valeur maximale avec le temps avant de décroître asymptotiquement vers 0.

Nous considérons ensuite le cas $A = 0$ où le détachement des particules solides est uniquement (ou plutôt principalement) provoqué par les collisions entre les particules mobiles et les particules fixes. Nous retrouvons alors les résultats du processus de renard (érosion régressive) obtenus par Vardoulakis et al (1996). Nous étudions les effets du coefficient d'érosion $B = 10$, 15 et 20, respectivement. Contrairement à une porosité qui demeure spatialement uniforme dans le cas de la suffusion, nous obtenons maintenant une porosité qui augmente simultanément dans le temps et dans la direction de

l'écoulement. En d'autres termes, nous sommes en présence d'une érosion qui progresse de l'aval vers l'amont, ce qui représente un processus de renard. Cette variation spatiale de la porosité est essentiellement due au fait que le taux d'érosion dans ce cas est proportionnel à la concentration de particules érodées qui devrait forcément augmenter de l'amont vers l'aval.

Le cas où les deux mécanismes d'érosion, fluide-particule et particule-particule, se présentent successivement (ou simultanément) est étudié pour différentes combinaisons des paramètres, A = 0.01, 0.1, 1 et B = 15. Les résultats obtenus montrent que la suffusion peut fortement influer sur le développement du processus de renard. Elle peut accélérer la formation d'un conduit (*piping*), d'environ 10h à 1 h lorsque A est augmenté de 0.01 à 1.

Lorsqu'un conduit est formé par l'effet de renard, il peut être élargi jusqu'à l'effondrement du barrage sous l'effet des contraintes hydrauliques et structurales. L'évolution du rayon du conduit sous l'effet des forces de cisaillement est étudié en se basant sur un une équation analogue à celles de Fell et al (2004) et Bonelli et al (2007), soit

$$r_{er} = k_{er}\tau_c\left(\frac{\tau}{\tau_c}-1\right)^n$$

où n est un paramètre de corrélation.

L'évolution temporelle du conduit est ainsi déterminée jusqu'à ce que le rayon du conduit atteigne la limite de rupture, pour trois valeurs de n = 0.5, 0.7 et 1.

Les résultats sont résumés au chapitre 5. Nous pouvons alors conclure que le modèle développé dans ce mémoire est capable de décrire l'évolution du phénomène d'érosion interne sous différentes conditions. Il faut noter que le modèle proposé ne peut pas prédire la rupture des barrages, mais nous permet de mieux comprendre un phénomène très complexe et d'avoir une nouvelle perspective de recherche vers un modèle plus réaliste.

TABLE OF COTENTS

LIST OF TABLES

LIST OF FIGURES

LIST OF SYMBOLS

A: constant parameter

A_s: specific surface [m^2/m^3]

A_t: total surface area of the pores [m^2]

b: experimental parameter

c: non-dimensional experiment parameter

C: concentration of transported particles

C_0: initial concentration of transported particles

C_u: coefficient of uniformity

d: diameter of particle [m]

d_i: particle diameter larger than i % by masse of the soil [m]

F_c: cohesive force [N]

F_D: drag force [N]

F_w: buoyant weight of particle [N]

g: Earth's gravity (9.81 m/s^2)

g_c: granulometry coefficient

i: hydraulic gradient

I: rate index

i_{crit}: critical hydraulic gradient

k: intrinsic permeability [m^2]

k_0: coefficient of intrinsic permeability [m^2]

k_D: Darcian coefficient of permeability

k_d: shape factor for drag force

k_{er}: erosion coefficient [s/m]

k_l: shape factor for lift force

k_w: shape factor for buoyant weight

L: length of the pipe [m]

M: momentum of sphere [kgm/s]

M_w: weight of water [kg/m^3]

M_p: weight of transported particles [kg/m^3]

M_s: weight of solid phase [kg/m^3]

n: correlative coefficient

N_e: number of erodible particles

q: flow rate or Darcy velocity [m/s]

r: radius of sphere [m]

R: radius of the pipe [m]

R_0: initial radius of the pipe [m]

Re: Reynolds number

r_{er}: rate of erosion per unit surface area [kg/sm^2]

$R_{collapse}$: estimation of the maximum radius before collapse of the roof [m]

R_{min}: minimum initial radius of the pipe [m]

S: rate of erosion per unit volume of porous medium [kg/sm^3]

S_D: rate of erosion due to viscous drag [kg/sm^3]

S_M: rate of erosion due to momentum transfer [kg/sm^3]

t: time [s]

V: volume element [m^3]

V_e: volume of erodible particles [m^3]

V_n: volume of non-erodible particles [m^3]

V_p: volume of transported particles [m^3]

V_s: volume of solid [m^3]

V_v: volume of voids [m^3]

V_w: volume of water [m^3]

v or v_w: interstitial velocity of flow [m/s]

$\overline{v}$: mean velocity of flow [m/s]

v_p: velocity of transported particles [m/s]

v_s: velocity of solid phase [m/s]

x: location in direction x [m]

Greek symbols

a: experimental parameter

α_d: inclination of the flow against vertical downward

γ_s: specific weight of soil [N/m^3]

γ_w: specific weight of water [N/m^3]

ΔP: pressure drop between upstream and downstream [Pa]

Δt: time step [s]

λ: coefficient of erosion [m^{-1}]

λ^*: effect factor of neighbouring particles

μ: dynamic viscosity of fluid

μ_0: initial dynamic viscosity of fluid

$\overline{\mu}$: dynamic viscosity of mixture

ρ_0: initial density of fine particles [kg/m^3]

ρ_d: dry density of soil [kg/m^3]

ρ_s: density of particle [kg/m^3]

ρ_w: density of water [kg/m^3]

$\overline{\rho}$: density of mixture [kg/m^3]

$\overline{\rho}_p$: apparent density of transported particles [kg/m^3]

$\overline{\rho}_s$: apparent density of solid phase [kg/m^3]

$\overline{\rho}_w$: apparent density of water [kg/m^3]

ϕ: porosity

ϕ_0: initial porosity

ϕ_{max}: maximum porosity

ϕ_i: porosity of i^{th} unit cell

Φ: friction angle

τ_w: shear stress at the wall [Pa]

τ_c: critical shear stress [Pa]

LIST OF APPENDICES

INTRODUCTION

Embankment dams are water barriers constructed of earth and rock. They are the most common type of dams used to impound water for a variety of purposes such as water supply, irrigation, navigation and power generation. Although the benefits of impounding water with a hydraulic structure such as a dam is obvious, its failure will generally lead to catastrophic consequences such as the loss of life and property. The two principal causes of failure in an embankment dam is due to prolonged overtopping at the crest or by uncontrolled internal erosion leading to a phenomenon known as 'piping'. The work in this thesis is confined to a study of the latter: the internal erosion process in embankment dams.

The generally accepted failure scenario for internal erosion in an embankment may be described as a process by which particles that may be susceptible to erosion from the interior of the dam are transported downstream by the seepage flow. If sufficient (generally very fine) particles are removed in this fashion, the seepage will increase followed by further transport of erodible particles and so forth, resulting in an acceleration of the process until most, if not all of the erodible particles have been washed out. The generally high pressure gradient across the dam body or foundation sustains this process. The removal of most if not all the fines results in the formation of an incipient 'pipe', which is basically a tunnel, or conduit between the upstream and downstream faces of the dam. The intensity of the seepage flow is now generally sufficient to remove all the remaining larger particles in the soil matrix remaining in the conduit resulting in 'piping'. Once formed, the pipe increases in diameter due to shear stress erosion along its perimeter. At the final stage of the process, part of the embankment above the pipe slumps into the flowing water creating a breach. In reservoirs of comparatively small volume, it has been frequently observed that due to the rapid drawdown of the water level, failure of the crest does not occur; nevertheless in almost all cases the reservoir is evacuated. The duration of the process from the start of increased seepage to a complete failure of the dam may vary from a few hours to many

years. The phenomena related to these mechanisms are often difficult to identify and to estimate.

To avoid embankment failure, early detection of internal erosion followed by remedial work is required. Methods that will contribute to the reliable assessment of the stability (risk analysis) of the dam need to be developed. Despite the large quantity of research activity in this field, much work remains to be done.

Objectives and Methodology

As stated earlier, the main objectives of this work are to understand the underlying mechanisms of internal erosion in embankment dams and to develop a mathematical model for the phenomenon. At the present time, it is generally accepted by experts in the field that the process consists of three stages: suffusion, backward erosion and progression. An attempt has been made in this thesis to develop a set of governing equations for the process based on physical considerations and to use numerical techniques to obtain the relevant solutions.

To achieve these objectives, the work has been laid out as follows:

- A review of existing results regarding internal erosion from field observations, experiments and modelling methods has been conducted.
- Construction of a mathematical model incorporating a choice of relevant parameters for the process.
- Use of numerical techniques to solve the governing equations.
- Analysis of the results obtained from the proposed model and comparison with those obtained in previous studies.

Limitations

For the sake of clarity in understanding a very complicated physical process, the numerical model developed in this work has been restricted to one space dimension and may therefore be considered as a first step towards the real situation where internal erosion is probably a three-dimensional problem. Moreover, at the present time, the influence of geological variables on the process is not well known so that not surprisingly, the use of several soil parameters is not incorporated into the model. Finally, realistic results regarding suffusion and/or backward erosion are unavailable at the present time, to permit extensive comparison and to fully asses the applicability of the proposed model.

Thesis Structure

This thesis is composed of five chapters.

Chapter 1 presents an overview of the phenomenon of internal erosion in embankment dams.

Chapter 2 discusses various existing models pertinent to the present work.

Chapter 3 details the development of the proposed model for internal erosion.

Chapter 4 is devoted to presentation of the results obtained by numerically solving the mathematical model for a set of parameters that have been used in some typical experiments. A critical discussion of the results is included.

Chapter 5 summarizes the results obtained and some perspectives for future research on the problem of internal erosion in embankment dams are presented in the conclusion.

CHAPTER I - INTERNAL EROSION IN EMBANKMENT DAMS

This chapter deals with embankment dams and internal erosion problems. The subject is only briefly introduced here, but other sources, for instance Fell (2005), present an excellent description of the erosion process in embankment dams. This section begins by providing some background information on embankment dams. Subsequently, problems associated with anomalous seepage and internal erosion are examined since such problems pertain to the body of work in this thesis.

1.1 Background

Based on the structure and material used, dams are classified as timber dams, arch-gravity dams, embankment dams or masonry dams. Today 70 – 80% of all dams is of the embankment type and includes the highest dam in the world (Fry, 2007).

Embankment dams may be subdivided into two main types, earth-fill and rock-fill.

Earth-fill dams are constructed of well-compacted earth, with some subtypes: homogeneous, modified homogeneous and zoned. The homogeneous type is composed of a single kind of material. In the modified homogeneous type, a drain layer is placed at the toe of the dam to collect the seepage water. The zoned type contains a central impervious core.

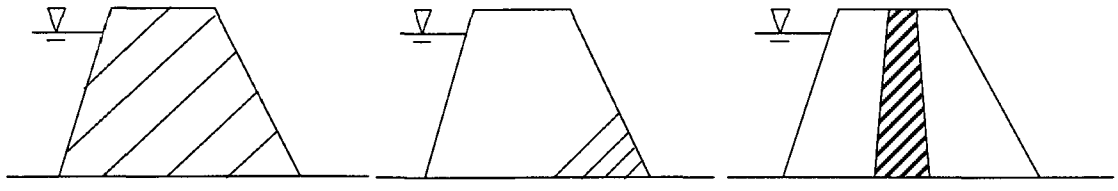

(a) Homogeneous (b) Modified homogeneous (c) Zoned

Figure 1.1: Types of earth-fill dams

Rock-fill dams are embankments of compacted free-draining granular earth with an impervious zone. Depending on the location of the impervious zone, rock-fill dams may be subdivided into three types: central core, sloping core and upstream core (Golzé, 1977).

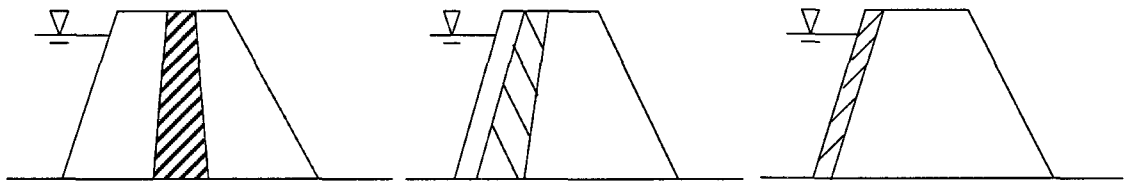

(a) Central core (b) Sloping core (c) Upstream exit core

Figure 1.2: Types of rock-fill dams

Embankment dams may be constructed from material found on-site or in close proximity; and for this reason they are very cost-effective. Many small embankment dams are built entirely of a single type of material such as stream alluvium, weathered bedrock or glacial till. Rock-fill types are suitable for larger embankment dams when there is no satisfactory raw material (earth) available and when a plentiful supply of sound rock is at hand.

Embankment dams are also suitable where the foundation has to be built on material which is far from ideal, especially when high hydrostatic uplift is likely to be a factor in the design.

Historically, embankment dams have been more susceptible to failure than other types of dams (Table 1.1).

From statistics compiled by the **I**nternational **C**ommittee **O**n **L**arge **D**ams (ICOLD) (1995), internal erosion has been a major cause of failure (Table 1.2). Further examination of the statistics reveals that failure through the embankment is twice as

common as failure through the foundation and 20 times as common as piping from the embankment into the foundation (Fry, 2007).

Table 1.1: Failure/year in the world (excluding China) from 1970 to 1990 – ICOLD 1995

Type	Number of dams	Number of failures	Rate of failures
Concrete or masonry	5500	2	2/100 000
Embankment	16500	26	9/100 000

Table 1.2: Failure rate in the world (excluding China) form 1970 to 1989 - ICOLD 1995

Modes of failure	Rate of failure 1970-1979	Rate of failure 1980-1989
Internal erosion	0.0020	0.0016
External erosion	0.0026	0.0019
Sliding	0.0004	0.0001

As seen from the ICOLD statistics above, most dam failures take place very early in the life of an embankment dam and frequently during the first filling of the reservoir.

1.2 Definitions

In order to clarify the presentation, the following definitions generally accepted in the literature (Fell and Fry, 2007), will be employed, unless otherwise indicated.

Internal erosion

Internal erosion is a phenomenon where soil particles within the embankment or the foundation of the dam are carried downstream by the seepage flow.

Concentrated leak erosion

Leaks within the embankment or the foundation of a dam may be caused by a crack due to differential settlement, desiccation, repeated freezing and thawing cycles or hydraulic fracture. The concentrated flow may cause erosion on the walls of the leak leading to enlargement of the leakage path. A concentrated leak may also arise in a continuous permeable zone containing coarse and/or poorly compacted materials.

Backward erosion

Backward erosion describes the process whereby soil particles are detached from the material matrix and transported downstream by the seepage flow. The process initiates with removal of particles at the downstream end and gradually progresses towards the upstream face of the embankment or the foundation until a continuous 'pipe' is formed.

Suffusion

Suffusion involves the selective erosion of fine particles from the intact soil skeleton composed of the coarser particles. The fine particles are removed through the voids between the larger particles by seepage flow, leaving behind the skeleton.

Heave

Heave (also known as 'blow out' or 'liquefaction') occurs in soils with little or no cohesion when seepage pore pressures are equal to total stress. Heave may often be followed by backward erosion if the seepage gradients remain high at the surface.

Piping

Piping is a state of internal erosion in which a continuous tunnel called a 'pipe' is formed completely between the upstream and the downstream side of the embankment or the foundation.

Soil contact erosion

Soil contact erosion involves the detachment of soil particles in the contact zone between two different soil layers.

Occasionally, the confusing term "suffosion" is encountered with the same meaning as 'soil contact erosion' or as 'backward erosion'; this is not the definition used here.

1.3 The Internal Erosion Process within an Embankment

The process of internal erosion may be represented by four phases: initiation of erosion, continuation (of erosion), progression to form a pipe and formation of a breach.

1.3.1 Initiation of erosion

Initiation is the first phase of internal erosion, where particles start to become detached. This may occur in four ways: by a concentrated leak, backward erosion, suffusion and soil contact erosion.

For a concentrated leak to initiate the process of particle detachment, the hydraulic shear stress along the walls of the concentrated leak must exceed the critical shear stress (i.e. the threshold value of shear stress which is sufficient to detach particles) of the soil.

For backward erosion, the seepage gradient at the exit point must be high enough to fluidize soil particles. This gradient is often less than the critical gradient required to cause heave. It follows therefore that if heave occurs, it is very likely that backward erosion will be initiated.

For suffusion, the seepage gradient must be high enough to move the fine particles within the coarse soil matrix. These hydraulic gradients are usually less than the critical gradient required to initiate backward erosion or heave.

1.3.2 Continuation

Continuation is the phase where the filter controls whether or not erosion will continue. There are four levels of progression from the 'no erosion' phase to the 'continuing erosion' phase.

1. No erosion: no soil particle can pass the filter.
2. Some erosion: some soil particles can enter the filter, but after this the filter clogs and seals, effectively halting the erosion process.
3. Excessive erosion: the base soil is eroded excessively but after this significant quantity of eroded soil the filter is sealed.
4. Continuing erosion: there is no filter or the filter is too coarse to prevent the movement of erodible particles from the dam.

1.3.3 Progression to form a pipe

Progression is the phase of internal erosion corresponding to the enlargement of the pipe due to particle removal along the perimeter resulting in an increase in pore pressure and seepage.

1.3.3.1 Progression of internal erosion initiated by a concentrated leak

Since the erosion cannot be limited, the flow hydraulics resulting from a concentrated leak will cause the erosion to progress, ultimately forming a pipe. The rate of erosion will depend on the hydraulic gradient and the geometry of the eroding leak as well as on the erodibility of the soil.

1.3.3.2 Progression of internal erosion initiated by backward erosion

In order for a pipe to be initiated by backward erosion, certain hydraulic criteria must be met.

(a) The seepage gradients at the downstream exit point must continue to exceed the critical gradient required to move particles.

(b) The flow velocity in the incipient pipe must be sufficient to erode and enlarge the pipe. Physically, there are two stages to consider:

i. Prior to the pipe being fully developed between the reservoir and the downstream end, the flow velocities are low.

ii. Once the pipe is fully developed, the hydraulic shear stresses will be larger and rapid progression is more likely to occur.

1.3.3.3 Progression of internal erosion initiated by suffusion

The process of internal erosion by suffusion involves the selective removal of the fine particles, leaving behind a (mechanically weaker) matrix of coarser particles. Erosion may progress to the extent that all the fine particles are eroded, without a pipe being formed.

For a pipe to develop, the seepage flow gradient subject to suffusion would have to exceed the critical value for backward erosion of the matrix of coarser particles. If so, the process develops as a backward erosion process.

1.3.4 Development of a breach

Internal erosion initiated by backward erosion or by erosion from a concentrated leak may form a breach by the following steps:

(a) Gross enlargement of a pipe.

(b) Local collapse of the pipe.

(c) Collapse of the whole pipe leading to crest settlement and overtopping of the embankment.

For internal erosion initiated by suffusion, a breach (without a pipe being formed) may occur due to the instability of the downstream slope.

1.4 Hydraulic criteria for internal erosion

1.4.1 Cohesionless soil

1.4.1 Critical gradient

Backward erosion

In cohesionless soil, hydraulic criteria for backward erosion are strongly related to the critical gradient for heave. Heave occurs when seepage pore pressure is such that the effective stress becomes zero. The critical gradient becomes

$$i_{crit} = \frac{(1-\phi)(\gamma_s - \gamma_w)}{\gamma_w} \tag{1.1}$$

where: γ_w is the specific weight of the water and γ_s is the specific weight of soil.

For a porosity of $0.25 \leq \phi \leq 0.48$ and a specific weight of the particles γ_s of 26 kN/m³ the critical gradient i_{crit} ranges between $0.83 \leq i_{crit} \leq 1.2$ (Perzlmaier et al., 2007).

Critical gradient values based on a large number of experimental trials for backward erosion at an unfiltered exit are presented in Table 1.3.

Table 1.3: Critical average gradients required to initiate backward erosion and form a pipe (ICOLD, 2007)

Soil	Gravel	Coarse sand	Medium sand	Fine sand
i_{crit} Chugaev	0.25	0.25	0.15	0.12
i_{crit} Chugaev reduced	0.25	0.25	0.11	0.10
i_{crit} after Bligh	0.11	0.083	-	0.037
i_{crit} after Lane	0.095	0.067	0.056	0.048
i_{crit} after Muller-Krichenbauer:				
lower limit	-	0.12	0.08	0.06
upper limit	-	0.17	0.10	0.08
i_{crit} after Weijers & Sellmeijer:				
$C_u = d_{60}/d_{10} = 1.5$	0.28	0.18	0.16	0.09
$C_u = 3$	0.34	0.28	0.24	0.14

Note that in this table, C_u is defined as the coefficient of uniformity

Suffusion

From Istomina (1957, in Busch et al. 1993) a hydraulic criterion for suffusion is presented as a function of the coefficient of uniformity C_u.

$$i_{crit} = \begin{cases} 0.3 \text{ to } 0.4 & \text{for } C_u < 10 \\ 0.2 & \text{for } 10 \le C_u \le 20 \\ 0.1 & \text{for } C_u > 20 \end{cases} \tag{1.2}$$

After Busch et al. (1993), the critical hydraulic gradients to initiate suffusion in soils that are not gap graded depends on the coefficient of uniformity C_u, the porosity ϕ, the dry density ρ_d, the Darcian coefficient of permeability k_D, the dynamic viscosity of the fluid μ and the inclination of the flow against vertical downward α_d.

$$i_{crit} = 0.6 \times \left(\frac{\rho_d}{\rho_w} - 1 \right) \left[0.82 - 1.8\phi + 0.0062 \times (C_u - 5) \right] \sin\left(30^0 - \frac{\alpha_d}{8} \right) \sqrt{\frac{\phi g d_s^2}{\mu k_D}} \tag{1.3}$$

d_s is the largest particle diameter subject to suffusion. It is about 0.6 times the mean pore diameter after Pavicic in Wittmann (1980).

$$d_s = 0.27 \sqrt[6]{C_u} \frac{\phi}{1-\phi} d_{17} \tag{1.4}$$

where d_{17} is the particle diameter larger than 17 % by mass of the soil. Other hydraulic criteria for suffusion have been given by Wittmann (1980) and by Muckenthaler (1989).

However due to the fact that dispersion of the underlying test results is very large, geometric criteria for suffusion are still rare unless they are very conservative. Accordingly, hydraulic criteria for suffusion still suffer from a lack of precision.

1.4.2 Cohesive soil

Basically, the critical erosion shear stress of cohesive sediments depends on the granulometry (i.e. particle size and shape) and cohesive particle content. The critical shear stress τ_c for the erosion of a spherical cohesive particle is

$$\tau_c = \frac{k_w \dfrac{\tan\Phi}{g_c k_d}}{d_c + \dfrac{k_l}{k_d}\tan\Phi\,\mathrm{Re} + \dfrac{3 d_c g_c}{16}\mathrm{Re}^2}\left(1 + \frac{F_c}{F_w}\right) \tag{1.5}$$

where Φ is the internal angle, F_c the cohesion force, F_w the buoyant weight of the particle, g_c the granulometry coefficient, k_d the shape factor for drag force, k_l the shape factor for lift force, k_w the shape factor for buoyant weight, Re the Reynolds number, and d_c the constant of drag coefficient (Bonelli et al., 2007).

1.5 Time for development of internal erosion in embankment dams

1.5.1 Time for initiation and the continuation phase

According to Fell and Fry (2007), it is not possible to separate the characteristic times for the two phases. Usual times for initiation and continuation in embankment dams are summarized in Table 1.4.

Table 1.4: Typical times for initiation and continuation in embankment dams

Mechanism	Usual time	Comment
Backward erosion	Slow to rapid/ very rapid	In the absence of a concentrated leak, it is slow. Otherwise it is rapid or very rapid. However, the final stage of initiation and continuation is likely to be rapid or very rapid.
Crack/hydraulic fracture	Rapid or very rapid	It is rapid when the reservoir level reaches the crack or reaches the level at which hydraulic fracture is induced.
High permeability zone	Slow to rapid	Rapid when the reservoir level reaches the high permeability zone and/or the critical gradients needed to initiate erosion are exceeded.
Suffusion/internal instability	Slow	The process involves a gradual migration of fines within the soil.

The time scales may be broadly defined as:

Slow: weeks or months, even years; Rapid: hours (>12h) or days; Very rapid: <3h

1.5.2 Time for progression to pipe formation and enlargement

There are many factors that influence this time; however, the rate of progression is independent of the mechanism of initiation. If the embankment is poorly compacted, partially saturated and the relative density is low, erosion will occur rapidly (or very rapidly). If not, erosion will occur at some intermediate rate.

If the upstream flow is limited by factors such as a fine grained or dirty rock-fill zone, or concrete facing, or if the potential for clogging of a crack by the filter material exists, the

progression time will be longer. In some cases, limiting of the flow may halt the erosion process, or perhaps reach equilibrium prior to breach of the dam.

1.5.3 Time for breach formation leading to failure

The time for breach development is difficult to separate from the progression phase. This time is largely controlled by the ability of the downstream zone to handle increased seepage flows. The two most important factors are permeability and erodibility of the material forming the downstream zone.

CHAPTER II - REVIEW OF EXISTING MODELS

A large amount of work has been done in an attempt to understand the processes of internal erosion in embankment dams. Several experimental methods were developed for testing the erodibility of soils with reference to the design of dams, preventing soil erosion and allowing for water seepage. Particular attention was focused on the influence of various factors, such as the seepage discharge, the confining pressure, and the concentration of moving particles, on the erosion rate and the critical shear stress. Along with the experimental works, some attempts have been made to model the phenomenon of erosion in a porous medium. The common goal of these studies is to describe the erodibility of a soil in terms of two principal factors, namely the ease of initiating erosion in the soil and the rate of erosion under a given shear stress. Basically, the constitutive equation of erosion, in conjunction with the transport equation of moving particles, constitutes the mathematical model of the phenomenon.

To set the stage for constructing a mathematical model that may describe both the suffusion and backward erosion processes, we will summarize in this chapter the most recent works on these phenomena. For a more exhaustive bibliography, we refer the reader to Fell (2005), Fry (2007), and Fell and Fry (2007).

2.1 Khilar and Fogler (1998)

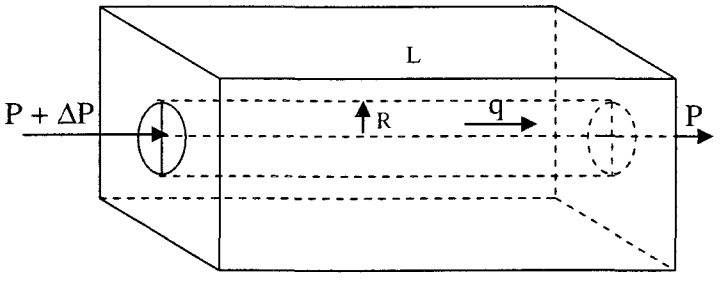

Figure 2.1: Schematic model of Khilar and Fogler

Khilar and Fogler (1998) adopted the following approach to solve the problem of migration of fines in porous media:

1) A capillary model to represent the geometry of the pore structure of the soil mass was postulated.
2) The increase in porosity due to erosion, and the consequent changes in the permeability and the flow rate were accounted for using the capillary model.
3) The soil erosion was assumed to occur entirely due to hydrodynamic forces. The wall shear stress will follow a linear dependence on flow velocity in laminar flow.
4) To further simplify the calculations, the concentration of particles was monitored until it reached a certain critical particle concentration. Beyond this point, it was assumed that soil erosion was halted due to entrapment of particles at the pore constrictions.

They found that typical values of the critical shear stress τ_c range from 0.10 to 2.0 Pa, typical critical flow velocities range from 0.01 to 0.1 m/s, and the rate of erosion may be expressed in the form

$$r_{er} = k_{er}(\tau_w - \tau_c) \tag{2.1}$$

where r_{er} is the rate of erosion per unit area of surface at the wall [kg/s.m^2], τ_w is the wall shear stress [Pa], τ_c is the critical shear stress [Pa], and k_{er} is the erosion rate coefficient [s/m] given by

$$k_{er} = 3\times10^{-8} - 17.1\times10^{-8}\tau_c + 40.2\times10^{-8}\tau_c^2 - 43.0\times10^{-8}\tau_c^3 + 17.5\times10^{-8}\tau_c^4 \tag{2.2}$$

2.2 Wan and Fell (2004)

These authors developed two sets of tests, namely the slot erosion test (SET) and the hole erosion test (HET) to study the erosion rate and critical shear stress of piping erosion in cracks and concentrated leaks in embankment dams.

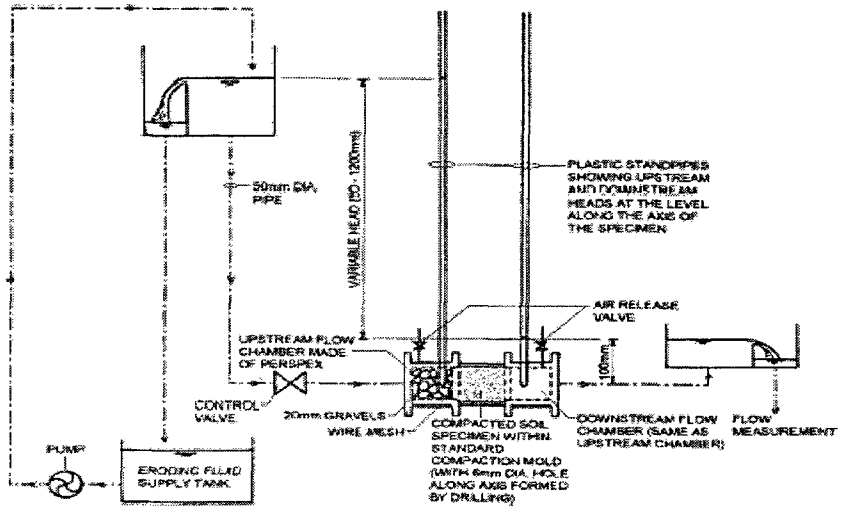

Figure 2.2: Schematic diagram of hole erosion test assembly

In the HET, as shown in Fig. 2.2, the soil specimen was compacted inside a standard mold with a 6 mm-diameter hole along the longitudinal axis of the soil sample to simulate a concentrated leak. The water head in downstream was set at 100 mm. The HET measured the flow rate to deduce the diameter of the hole.

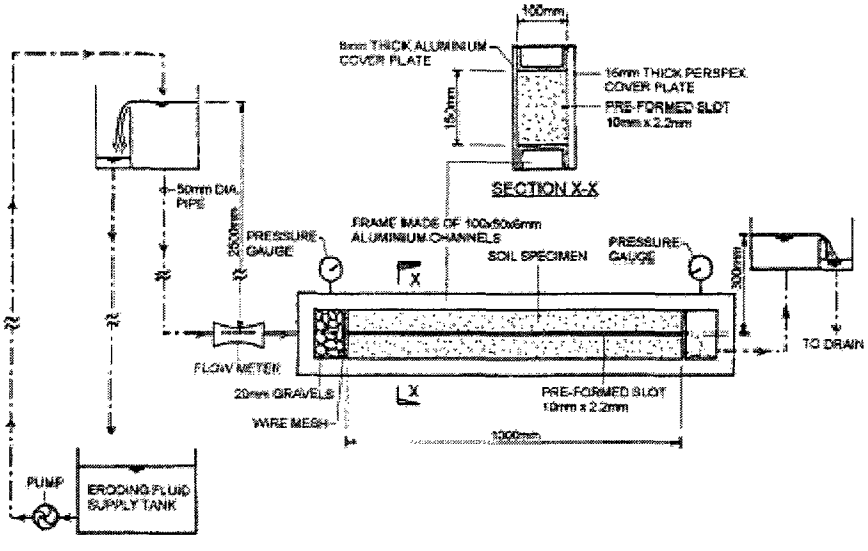

Figure 2.3: Schematic diagram of slot erosion test assembly

The setup of the SET, shown in Fig. 2.3, is similar to that of the HET, except a much larger soil specimen is compacted inside a 0.15 m wide x 0.1 m deep x 1 m long box, and the hydraulic gradient is set at 2.2. A 2.2 mm wide x 10 mm deep x 1 m long slot is formed along one surface of the soil sample. The discharge was measured at chosen time intervals.

The diameter of the hole in HET or the width of the slot SET was then deduced and the erosion rate was obtained from its time derivative.

The relationship between the rate of erosion and shear stress was expressed as

$$r_{er} = k_{er}\left(\tau_w - \tau_c\right) \tag{2.3}$$

where r_{er} is the rate of erosion per unit surface area of the slot/hole at time t (kg/s.m^2), k_{er} is the soil erosion coefficient (s/m), τ_w is the hydraulic shear stress along the slot/hole at time t (Pa) and τ_c is the critical shear stress (Pa).

Table 2.1: Summary of erosion rate indices and critical shear stresses

Soil sample	% fine	% clay	I_{SET}, I_{HET}	Range of I_{SET} or I_{HET}	τ_c
Rowallan	22	9	0.6, 1.0	<2	<6.4
Lyelle	29	15	1.6, 1.7	<2	<6.4
Teton	84	14	3.1, 2.4	2-4	12.8-25.6
Pukaki	42	17	3.5, 2.7	2-4	12.8
Jindabyne	34	18	3.3, 2.9	2-4	6.4-12.8
Bradys	75	60	3.4, 3.2	3-4	6.4-12.8
Waranga Basin	79	58	3.3, 3.8	3-4	51.2-64.0
Hume	81	59	4.2, 3.9	3-5	<64.0
Matahina	50	29	6.0, 3.8	3-6	10.3-127.9
Fattorini	75	20	4.4, 4.8	4-5	76.7-89.5
Waroona	61	52	5.9, 5.7	5-6	>153.5
Shellharbour	88	80	5.6, 5.8	5-6	102.3
Buffalo	87	59	>6, >6	>6	>153.5

As the erosion coefficient k_{er} obtained for various HETs and SETs, are small numbers, and since $-\log(k_{er})$ was often used in plotting the results, the authors have introduced the so-called erosion rate index I defined as

$$I = -\log\left(k_{er}\right) \tag{2.4}$$

I has an order of magnitude in the range of 0 to 6, describing soils that are extremely erodible to soils that are almost non-erodible. The obtained results are shown in Table 2.1.

2.3 Bonelli et al. (2007)

In this study, a series of tests were performed to quantify the rate of erosion of different soils in pipes of various diameters, and to provide an estimation of the remaining time to breaching of earth dams when piping erosion occurs.

The hole erosion test was designed to simulate piping flow in a hole. An eroding fluid is driven through the soil sample to initiate erosion along a preformed hole. The results were obtained in terms of the flow rate versus time. The flow rate was then used as an indirect measurement of the erosion rate. This latter was expressed in the form of the threshold equation

$$r_{er} = \begin{cases} 0 & \text{if} \quad \tau_w \le \tau_c \\ k_{er}\left(\tau_w - \tau_c\right) & \text{if} \quad \tau_w > \tau_c \end{cases} \tag{2.5}$$

where:

r_{er}: mass flux of eroded material (soil particles + water) crossing the interface (kg/sm^2)

τ_w: tangential shear stress at the interface (Pa)

τ_c: critical stress (Pa)

k_{er}: erosion coefficient (s/m)

The results are summarized in Table 2.2.

Table 2.2: Properties of soils samples, critical shear stress and erosion coefficient

Soil		Gravel (%)	Sand (%)	Fine (%)	<2μm (%)	τ_c (Pa)	k_{er} (10^{-4} s/m)
Bradys	High plasticity sandy clay	1	24	75	48	50-76	3-5
Fattorini	Medium plasticity sandy clay	3	22	75	14	6	8
Hume	Low plasticity sandy clay	0	19	81	51	66-92	0.3-3
Jindabyne	Clayey sand	0	66	34	15	6-72	3-9
Lyell	Silty sand	1	70	29	13	8	140
Matahina	Low plasticity clay	7	43	50	25	128	1
Pukaki	Silty sand	10	48	42	13	13	10
Shellharbour	high plasticity clay	1	11	88	77	99-106	0.5-3
Waranga	Low plasticity clay	0	21	79	54	106	1

It should be noted that the law of erosion suggested by Khilar and Fogler (1998) has the same form as that of Wan and Fell (2004) as well as that of Bonelli et al. (2007). They all assumed that the erosion rate is zero when the wall shear stress is below a critical value, and when all fines are removed, the porosity will remain unchanged and the rate of erosion will tend to zero.

The main differences in these studies lie in the suggested values of the erosion rate coefficient and the critical shear stress. The range of critical shear stresses suggested by Khilar and Fogler (1998) is very small compared with the minimum value of the other authors. Also, according to eq. (2.2), the erosion rate coefficient $k_{er} = 6.56\times10^{-7}$ s/m for a critical shear stress τ_c = 2 Pa. This value of k_{er} is very small compared with those of other authors. Many previous experiments indicated that the smaller the critical shear stress, the larger the erosion rate coefficient (the soil is more erodible). Therefore, the formula for the erosion rate coefficient in eq. (2.2) may not be very accurate.

2.4 Sterpi (2003)

The formulation of a law governing the erosion rate was deduced from the experimental results obtained by Sterpi (2003). The investigation involved laboratory tests performed on reconstituted samples of granular soil recovered from borings in the Milan [Italy] area. The granular soil, consisting of silty sand with a fine fraction of about 20% by weight, was compacted in layers of small thickness within a vertical pipe with internal diameter of 10 cm and height of about 14 cm.

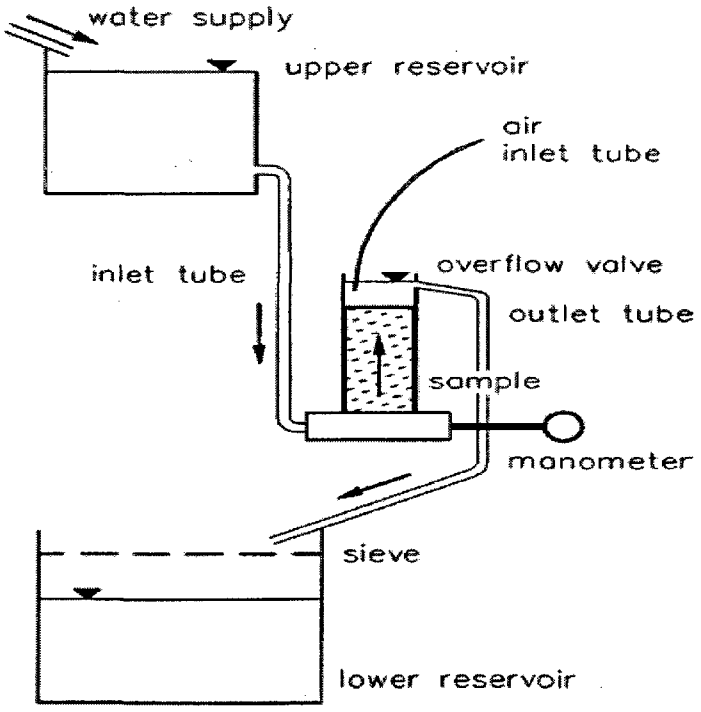

Figure 2.4: Experimental setup for seepage tests

The ''moist tamping'' technique was adopted to obtain the same initial relative density for all samples. After preparation the samples were subjected to the flow of water in the upward vertical direction, under a constant hydraulic head. Under the effect of internal erosion, fine particles leave the soil sample to be transported into the lower reservoir.

The density of the fine fraction in the samples decreases with time t during the erosion tests from its initial value ρ_0 to a final long-term value ρ_∞ ($\cong$0). The weight of fine particles leaving the test rig was recorded at regular time intervals. The dots in Figure 2.3 represent the experimental variation of the eroded density $\rho_0 - \rho_\infty$ (t) during time for four values of the imposed hydraulic gradient i.

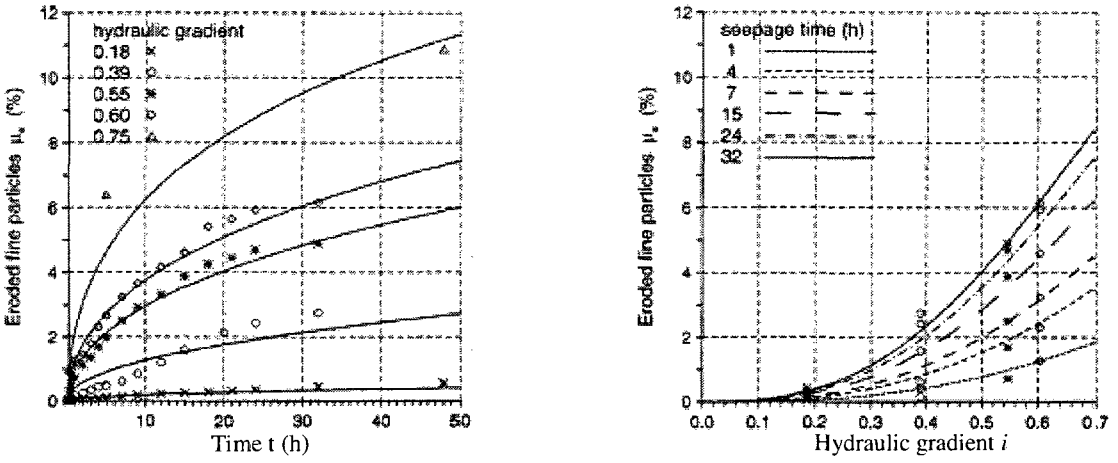

Figure 2.5: Variations in the percentage by weight of eroded fine particles with time (left) and with hydraulic gradient (right), from laboratory tests (dots) and from their analytical expression, eq. 2.6 (solid lines)

From the experimental results, the author has deduced the following empirical relation for the erosion rate:

$$S = \rho_0 \cdot \left(-\frac{b}{t_0}\right) \cdot \left(\frac{t}{t_0}\right)^{b-1} \cdot \frac{i^c}{a} \cdot \exp\left[-\left(\frac{t}{t_0}\right)^b \cdot \frac{i^c}{a}\right] \qquad (2.6)$$

where S is the rate of erosion per unit volume of porous medium [kg/m^{3}s], ρ_0 is the initial density of fine particles [kg/m^3], t_0 = 1h, a, b, c are non-dimensional experimental parameters, t is time [h], and i is the hydraulic gradient.

We note from the above relation that the erosion rate is a function of the hydraulic

gradient and time. As the hydraulic gradients were kept constant in these tests, it follows that S is only a function of time. We therefore deduce that it may just be valid in the case of suffusion.

2.5 Bendahmane (2005)

Bendahmane developed a triaxial device to study the initiation of suffusion and backward erosion for sandy-clay samples (Figure 2.6).

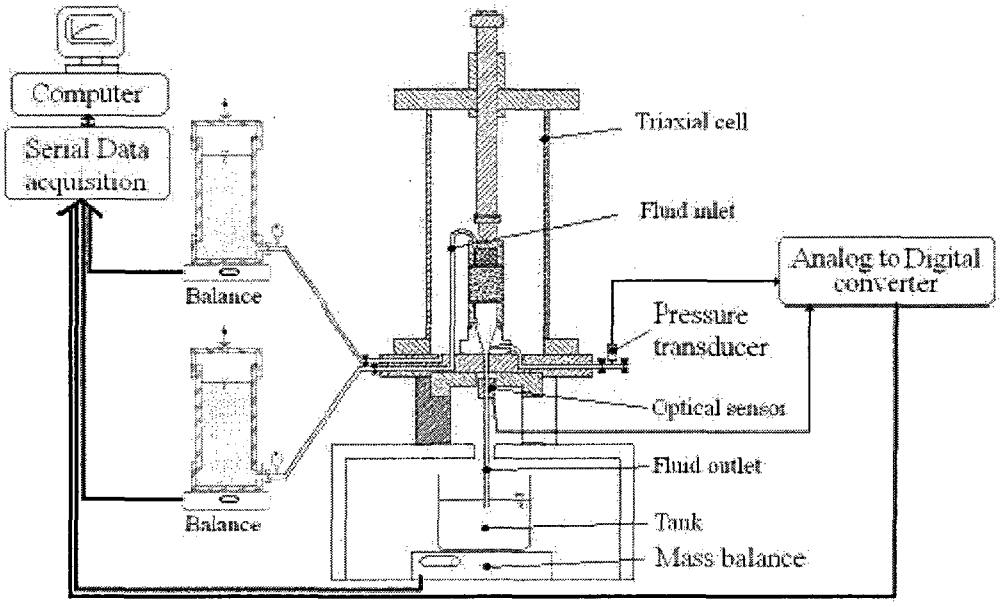

Figure 2.6: Schematic representation of the experimental triaxial cell.

The device was placed in a temperature-controlled chamber (20 ± 0.5°C) and consists of three modified triaxial cells. These cells have been modified to let the flow come up to the core of the sample. So as to avoid all unwanted disturbances on the samples, saturation, consolidation, hydraulic and mechanical test stages were carried out inside the same cell without de-confining the samples. The realization of long-duration tests was possible thanks to the automation of both the monitoring and the data acquisition. The use of three cells simultaneously made it possible to reduce the duration of the test program.

The detection of erosion in the effluent was performed using optical aids and by weighing the amount of grains in the eroding fluid. The critical gradient for internal erosion may be assessed from the effluent instantaneous optical analysis. In order to track the development of internal erosion, injection volume flow rates and obtained mass flow rate measurements were compared.

Based on the law of erosion of Papamichos et al. (2001), and on his own experimental results, Bendahmane (2005) proposed the following expression for the rate of erosion:

$$S = \rho_s \lambda \frac{(1-\phi)}{\phi} q \tag{2.7}$$

where S is the rate of erosion per unit volume of porous medium [kg/m^3-s], ρ_s is the density of solid, λ is the erosion coefficient [m^{-1}], ϕ is the porosity. A comparison between theoretical and experimental results are shown in the following figures for a sample with 10% of clay, restricted by 200 kPa with a hydraulic gradient 20m/m, an initial permeability $k_0 = 3\text{x}10^{-5}$ m/s, an initial porosity $\phi_0 = 0.33$, and a coefficient of erosion $\lambda = 0.001$ m^{-1}.

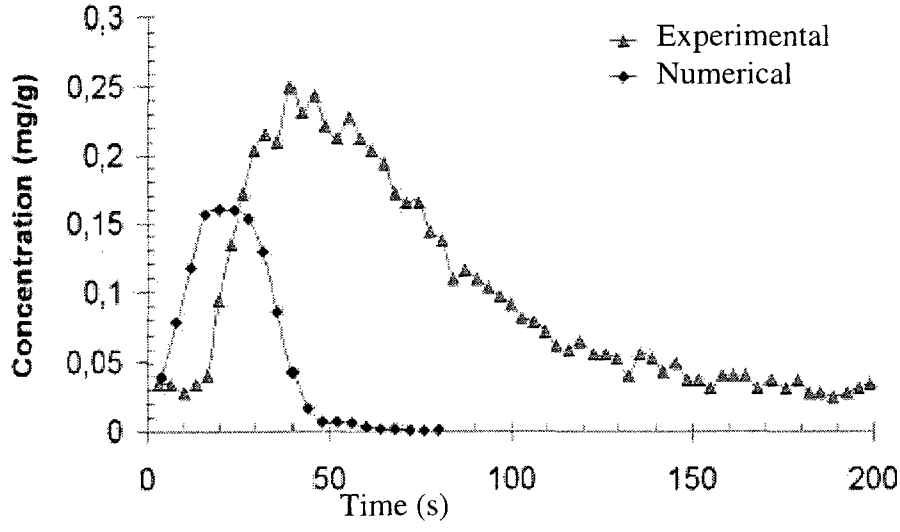

Figure 2.7: Time evolution of concentration of outflow

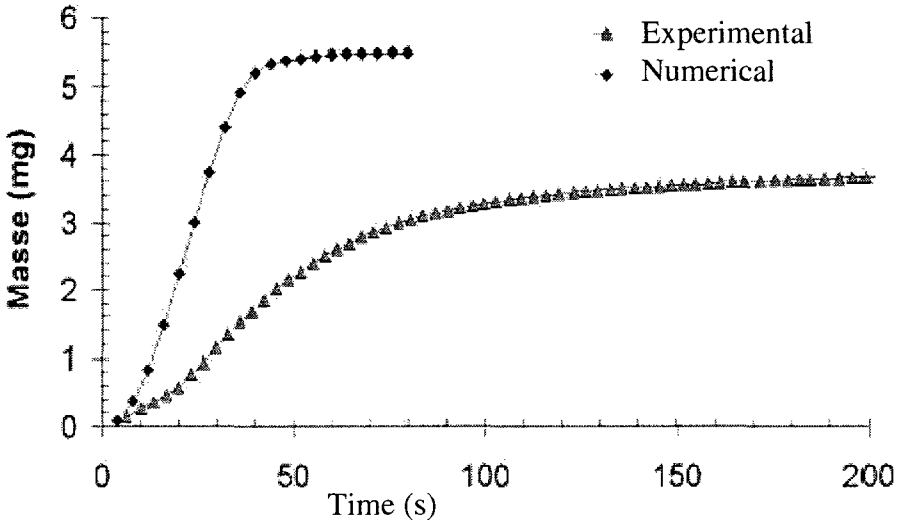

Figure 2.8: Time evolution of total eroded mass outflow

From these results it appears that the porosity of the soil remains spatially uniform, and this law of erosion may only describe the phenomena of suffusion.

2.6 Vardoulakis et al. (1996)

Based on the experimental and theoretical studies in relation with the filtration of solid particles by Hughes (1954), these authors assumed that the rate of erosion is proportional to the concentration of transported particles in the filtration flow. Moreover, the erosion process was expected to be more intense in intact regions, which are characterized by smaller pore channels. They therefore proposed the following constitutive equation for the erosion rate:

$$S = \rho_s \lambda (1-\phi) C q \tag{2.8}$$

where S is the rate of erosion per unit volume of porous medium [kg/m^{3}s], ρ_s is the solid density, λ is the coefficient of erosion [m^{-1}], ϕ is porosity and C is the volumetric concentration of transported particles.

The problem of fluid flow and particle erosion was then solved for the following set of numerical values assigned to the parameters:

- Specimen length $L = 1$ m
- Erosion coefficient $\lambda = 10\ m^{-1}$
- Initial porosity $\phi(x, 0) = \phi_0 = 0.25$
- Starting transport concentration $C(x, 0) = C_0 = 10^{-4}$
- Draw-down pressure $\Delta P = P_L - P_0 = 10$ MPa
- Initial permeability $k\ (x, 0) = 27.8$ mD

The results obtained for C, ϕ and q are shown in the following figures.

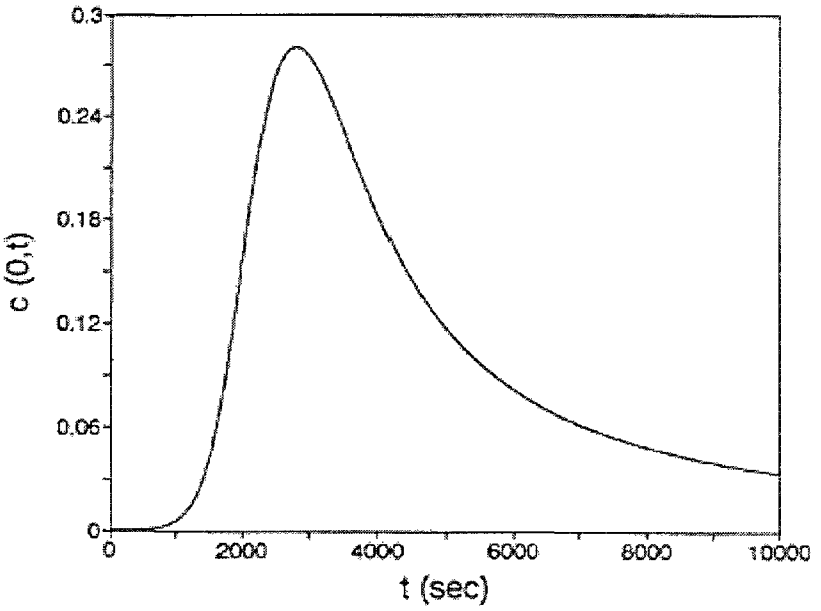

Figure 2.9: Time evolution of particle concentration at exit point

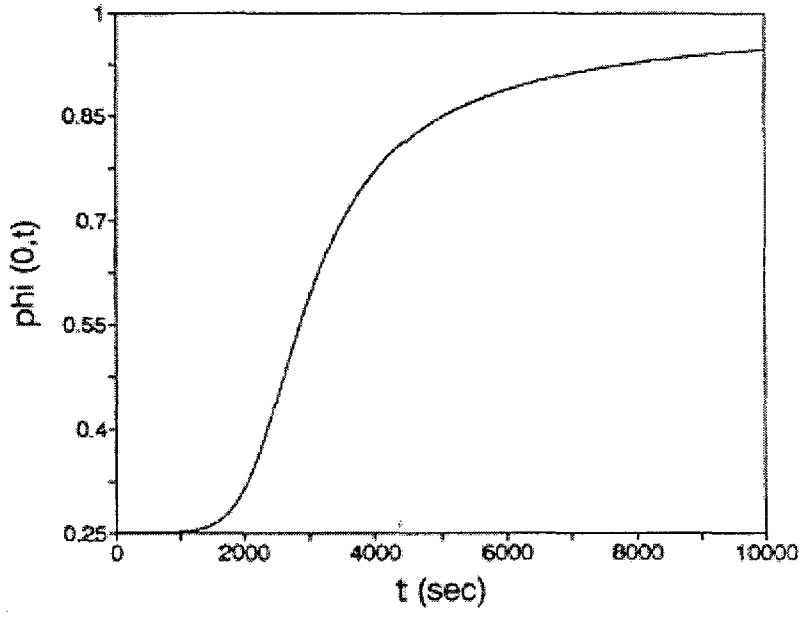

Figure 2.10: Time evolution of porosity at exit point

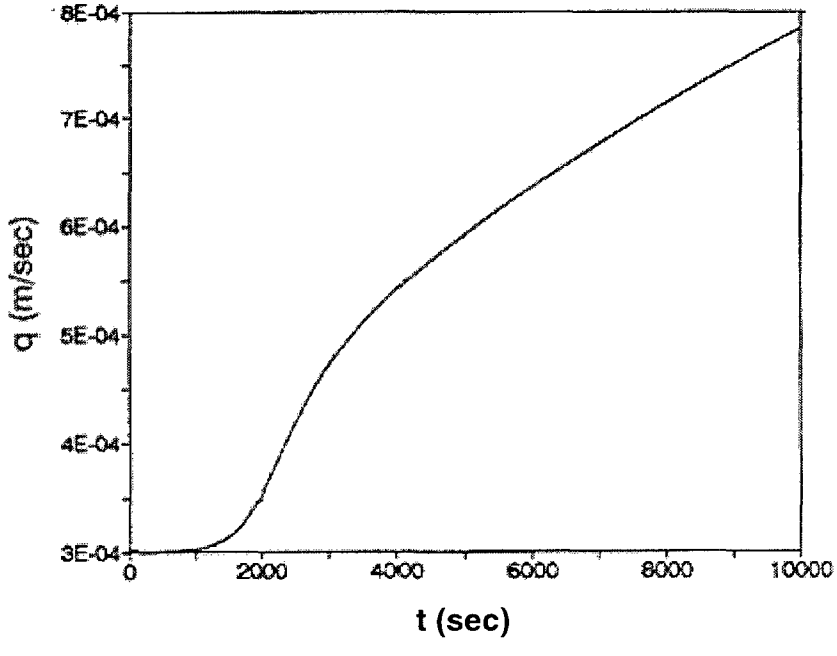

Figure 2.11: Time evolution of fluid discharge at exist point

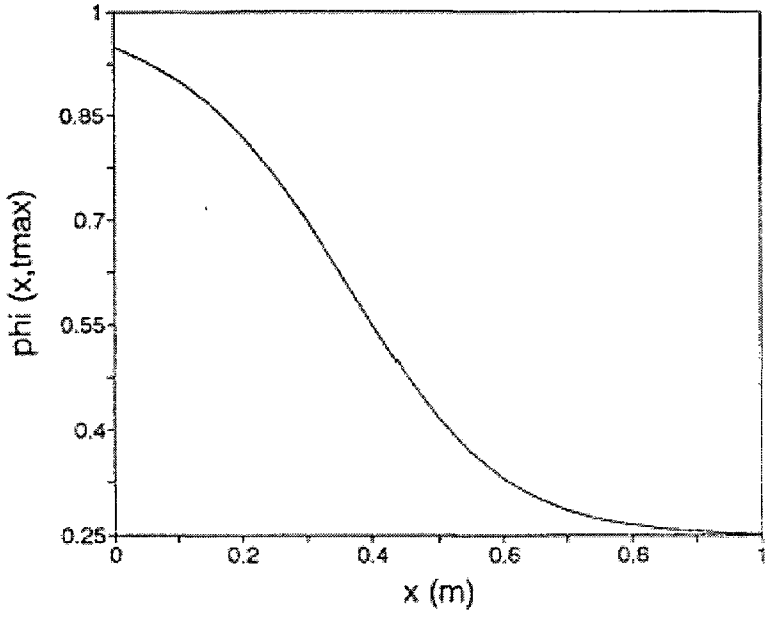

Figure 2.12: Spatial profile of porosity at 10^4 sec

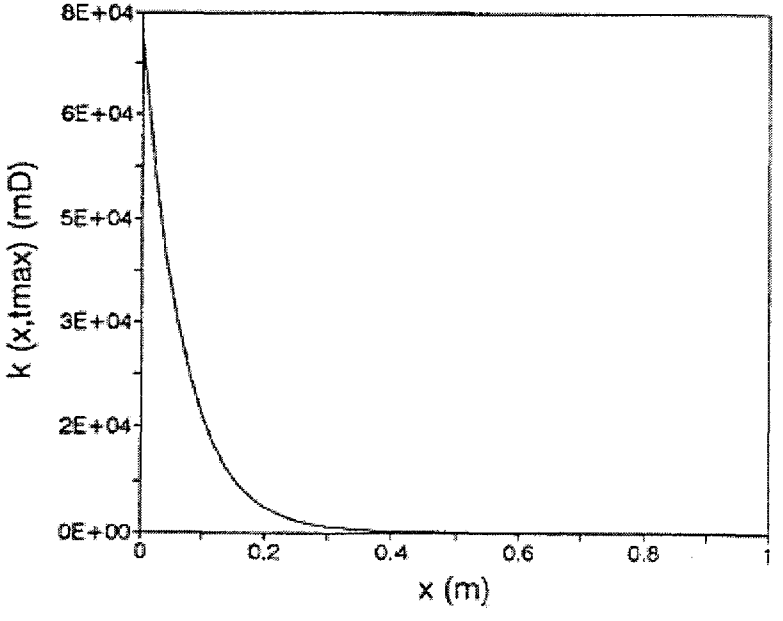

Figure 2.13: Spatial profile of permeability at 10^4 sec

From these results, it appears that under the effect of erosion, the porosity of the porous medium increases in time as well as in space (in the downstream direction). This may therefore correspond to the phenomenon of backward erosion.

It is worth noting that the above constitutive equation has been deduced from the argument that the concentration of moving particles may strongly affect the erosion rate via the variations in the viscosity of the fluid-particle mixture as shown in the work of Hughes (1954).

In summary, we may conclude from these studies that:

- The experimental results were obtained from tests on a limited number of soil samples. The results may be useful for those samples under certain conditions; however the applicability of the results for other conditions and other soil samples cannot be assured.

- There is no integrated model that examines all stages of internal erosion, from initiation to final collapse.

However, using these methods as a starting point, with incorporation of some useful experimentally determined parameters, it is possible to construct a model for the process, obtain (numerical) results and compare them with results available in the literature, as will be presented in the following chapters.

CHAPTER III - MATHEMATICAL MODEL OF INTERNAL EROSION

3.1. Physical description

For the purpose of the present study, embankment dams will be modeled as being composed of a granular porous medium through which water may flow as a consequence of a pressure difference ΔP (between upstream and downstream) in the flow direction. The porous medium representing the dam is composed of two types of particles, "fine" and "coarse". The coarse particles make up the skeleton of the medium while the fine particles are thought to be dispersed throughout the voids between the coarse particles.

It has been well recognized that the phenomenon of internal erosion may be divided into three stages:

(1) Suffusion is the first stage during which all the fine particles that are lodged in the spaces between the large particles are removed from the system by the seepage flow.

(2) Backward erosion is the next stage where all the coarse particles constituting the remaining skeleton matrix are removed progressively from the downstream to the upstream end resulting in the formation of an empty *'pipe'*,

(3) The mainly liquid flow through the pipe now passes relatively unhindered resulting in enlargement of the pipe until a breach is formed; this being the terminal stage.

Let us now consider a volume element V within the porous medium. The volume consists of three components: fixed solid particles (s), flowing water (w) and moving (eroded) particles (p) with masses M_s, M_w, M_p and volumes V_s, V_w, V_p.

Note that hereafter, the properties of solid particles, water and eroded particles will be designated with subscripts s, w and p, respectively.

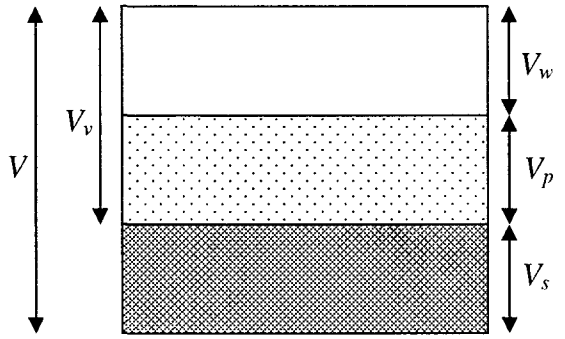

Figure 3.1: A volume element of a porous medium

Let the void space V_v be filled with a volume of fluid V_w and a volume of eroded particles V_p. We thus have

$$V_v = V_w + V_p \tag{3.1}$$

and

$$V = V_v + V_s \tag{3.2}$$

Transported particles are eroded particles in suspension and move within the void space. For simplicity, it may be assumed that the (liquid) water and transported particles have the same velocity, while the solid matrix is constituted of fixed particles. In other words, a particle having a zero velocity belongs to the solid matrix while those who move with the fluid are considered as eroded particles (i.e. $v_s = 0$, $v_w = v_p = v$).

In order to describe the fluid flow and erosion process within a porous medium, it is necessary to define the following quantities and parameters.

Specific surface

The *specific surface* A_s of a porous medium is defined as the total surface of the pores (A_t) per unit volume of porous medium (V):

$$A_s = A_t / V \tag{3.3}$$

For a porous medium made up of spheres of radius r packed cubically, we have

$$A_s = 4\pi r^2 / (2r)^3 = \pi / 2r \tag{3.4}$$

which indicates that fine particles exhibit a much higher specific surface than coarse materials. For example, the specific surface of sand may vary from 150 to 220 cm^{-1}.

Noting that the porosity in a cubical packing is $\phi = 1 - \pi/6$, we obtain

$$A_s = 3(1-\phi)/r \tag{3.5}$$

In general the specific surface of a porous medium depends on the porosity, the mode of packing as well as the size and shape of the grains. For example, disc–shaped particles exhibit a much larger specific area than spherical ones.

Densities

Density of water:

$$\rho_w = \frac{M_w}{V_w} \tag{3.6}$$

Density of transported particles:

$$\rho_s = \frac{M_p}{V_p} \tag{3.7}$$

Density of the mixture:

$$\bar{\rho} = \frac{M_w + M_p}{V_v} = (1-C)\rho_w + C\rho_s \tag{3.8}$$

Apparent density of eroded particles (mass of eroded particles within a unit volume of porous medium):

$$\bar{\rho}_p = \frac{M_p}{V} = \rho_s \frac{V_p}{V} = \rho_s \frac{C\phi V}{V} = C\phi\rho_s \tag{3.9}$$

Apparent density of solid phase:

$$\bar{\rho}_s = \frac{M_s}{V} = \rho_s \frac{V_s}{V} = \rho_s \frac{V - V_v}{V} = (1-\phi)\rho_s \tag{3.10}$$

Apparent density of water:

$$\bar{\rho}_w = \frac{M_w}{V} = \rho_w \frac{V_v - V_p}{V} = (1-C)\phi\rho_w \tag{3.11}$$

Porosity

The volumetric porosity is defined as

$$\phi = \frac{V_v}{V} \tag{3.12}$$

We may assume that the volumetric porosity is the same as the cross-sectional (or surface) porosity.

Concentration of eroded particles

The *volumetric concentration* C of the eroded particles within the void space is defined as

$$C = \frac{V_p}{V_v} \tag{3.13}$$

Then the volume occupied by eroded particles within a unit volume of porous medium is

$$\frac{V_p}{V} = \frac{V_p}{V_v}\frac{V_v}{V} = \phi C \tag{3.14}$$

so that the mass of eroded particles within a unit volume of porous medium is

$$\rho_s \phi C \tag{3.15}$$

Specific discharge rate, filtration velocity, Darcy velocity and interstitial velocity

The specific discharge rate q of the flow is the volume of water passing through a unit surface during a unit time (m^3/sm^2). It is thus equal to the average velocity (m/s), also called the filtration or Darcy velocity. As the flow is limited to the pore space, the velocity v of water within the pore space is related to the specific discharge rate q by

$$v = \frac{q}{\phi} \tag{3.16}$$

which is also called the local or interstitial velocity.

3.2 Equation of mass conservation

Let S be the net mass eroded per unit time, in a unit volume of porous medium, at a given time and position.

For the sake of simplicity, we shall restrict our study to 1-D flows, and we shall neglect the effects of mass diffusion.

We then have the following equation of mass conservation of the solid phase:

$$\frac{\partial \overline{\rho}_s}{\partial t} + \frac{\partial (\overline{\rho}_s v_s)}{\partial x} = -S \tag{3.17}$$

Replacing (3.10) and $v_s = 0$ into (3.17), we readily have:

$$\frac{\partial \left[(1-\phi)\rho_s\right]}{\partial t} = -S \tag{3.18}$$

i.e.
$$\frac{\partial \phi}{\partial t} = \frac{S}{\rho_s} \tag{3.19}$$

For eroded particles, we have the following equation of mass conservation:

$$\frac{\partial \overline{\rho}_p}{\partial t} + \frac{\partial (\overline{\rho}_p v_p)}{\partial x} = S \tag{3.20}$$

Replacing (3.9) and (3.16) into (3.20), we have:

$$\frac{\partial (C\phi)}{\partial t} + \frac{\partial (Cq)}{\partial x} = \frac{S}{\rho_s}$$

i.e.
$$\frac{\partial (C\phi)}{\partial t} + q\frac{\partial C}{\partial x} = \frac{S}{\rho_s} \tag{3.21}$$

Finally the mass conservation equation for water is

$$\frac{\partial \overline{\rho}_w}{\partial t} + \frac{\partial (\overline{\rho}_w v_w)}{\partial x} = 0 \tag{3.22}$$

Replacing (3.11) and (3.16) into (3.22), we obtain

$$\frac{\partial \left[(1-C)\phi\right]}{\partial t} + \frac{\partial \left[(1-C)q\right]}{\partial x} = 0$$

i.e. $$\frac{\partial(C\phi)}{\partial t}+q\frac{\partial C}{\partial x}=\frac{\partial \phi}{\partial t} \tag{3.23}$$

3.3 Equation of fluid flow

Many approaches have been proposed to derive the equation of fluid flow in porous media. All these approaches lead to the conclusion that the pressure and gravity forces are balanced by the viscous force which is proportional to the filtration velocity. We thus have the following equation for one-dimensional flows (along the x direction)

$$q=-(k/\mu)(dP/dx+\rho g dz/dx) \tag{3.24}$$

which is usually referred to as the Darcy law who first discovered it experimentally in 1856.

The above equation may be expressed as

$$q=-k(\rho g/\mu)dh/dx \tag{3.25}$$

where the piezometric head h, defined as $h = z+P/\rho g$ and measured in meters of water, is the sum of the pressure and potential energy of the fluid per unit weight, and $-dh/dx$ is the hydraulic gradient, usually denoted by i.

The Darcy law for fluid flow in porous media may be derived using different models. The most familiar models used in deriving the Darcy law are the capillary tube model and the flow resistance model. The development of these two models is summarized in the Appendix.

It should be noted that as the permeability k depends essentially on the geometry of the pore system, different models lead to different relations between the permeability k and the porosity ϕ, but they all show that the filtration velocity depends linearly on the pressure gradient as observed in Darcy's experiments.

In fact, while the capillary tube model and the flow resistance model respectively give $k=\phi R^2/8$ and $k=\pi\phi^2/6\lambda(1-\phi)d^2$, a model proposed by Carman-Kozeny where the

porous medium is represented as a network of interconnected channels or passages, leads to the well-known formula (see, e.g. Bear 1972)

$$k = \frac{d_m^{\,2}}{180}\frac{\phi^3}{(1-\phi)^2} \tag{3.26a}$$

where d_m represents some mean particle size which is defined as $d_m = 6\frac{V_s}{A}$ with A being the surface of the voids (or of the solid particles) and V_s the volume of the solid particles.

It should be noted that this formula was derived for a porous medium as being a system of interconnected channels with some hydraulic diameter R defined as the ratio of the volume of a conduit filled with a fluid to its perimeter, i.e.

$$R = \frac{\phi V}{A_t} = \frac{\phi V}{A_o + A} = \frac{\phi}{1/R_0 + 6(1-\phi)/d_m} = \frac{d_m \phi}{6[d_m/6R_o + (1-\phi)]} \tag{3.26b}$$

where a hydraulic diameter $R_o = \frac{V}{A_o}$ has been introduced, with A_o being the perimeter of the porous '*pipe*' and V being its volume.

If the porous matrix in this '*pipe*' is washed out, water will flow through this empty pipe with a hydraulic radius R_o. We may therefore use the following generalized formula for the permeability for ϕ varying from 0 to 1:

$$k = k_0 \frac{\phi^3}{\left[(1-\phi) + \frac{\sqrt{2k_o}}{R_o}\right]^2} \tag{3.26c}$$

This formula is practically the same as that of Carman-Kozeny for $\phi < 1$ while it reduces to that of an empty pipe when $\phi = 1$.

3.4 Equation for erosion rate

A fluid flowing through a porous medium exerts a force on the solid matrix that has important effects on the process of internal erosion.

According to Terzaghi (1967), three types of force act upon the solid particles of the porous medium: the weight of the solids acting in a downward direction, the buoyancy force which is the resultant of the liquid pressure, and the viscous or shear force acting at the solid-liquid interface.

The total force acting on the solid particles in a porous media may loosen these particles from their fixed position in the porous structure. These particles may be detached (leaving behind a local cavity), to be eventually washed out of the porous medium.

As shown in the previous chapter, Bendahmane et al. (2005) have proposed that the erosion rate of fine particles in a porous matrix is directly proportional to $q(1-\phi)/\phi$ while Vardoulakis and co-workers (1996) have found that the erosion rate should vary as $q(1-\phi)C$ where C is the concentration of eroded particles. According to the erosion rate found by Bendahmane et al. (2005) the porosity of the medium would remain spatially uniform during the whole process. This may be true only during the so-called suffusion process. From the erosion rate equation proposed by Vardoulakis (1996), the porosity of the medium must increase in the downstream direction. (Also note that if the concentration C is zero, then no erosion is predicted). This non-uniform erosion may occur in the so-called backward erosion process where a 'tunnel' could gradually make its way upstream from the exit (downstream) point of the water into the interior of the dam. To unify these two situations, the key question is to find a model equation for the rate of erosion in terms of the most significant parameters of the problem. The approach adopted in this work, is to construct a model of internal erosion by considering the fluid-particle and particle-particle interactions as two eroding mechanisms occurring simultaneously. The shear force effects of the interstitial flow on the erosion rate of the soil structure are considered first. Subsequently, these suspended particles detached from the soil structure and transported by the flow may have the effect of successfully dislodging, by collision, additional particles bound to the exposed soil structure. A combination of these two mechanisms of erosion, namely the fluid-particle interactions

and the particle-particle interactions, should lead to a mathematical model that may describe the suffusion as well as the backward erosion phenomena.

Let us therefore consider a unit volume (V = 1 m^3) of porous medium comprised of two fractions of solid particles: 'erodible' and 'non-erodible' occupying a volume V_e and V_n, respectively, as shown in the figure below.

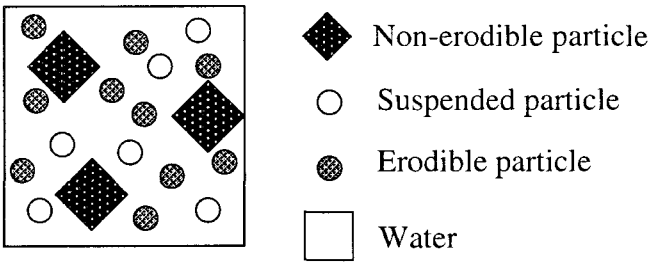

Figure 3.2: A unit volume of porous medium

The void volume within this porous element is

$$V_v = V - (V_e + V_n) = 1 - (V_e + V_n) \tag{3.27}$$

and the porosity of V is

$$\phi = \frac{V_v}{V} = \frac{V - (V_e + V_n)}{V} = 1 - (V_e + V_n) \tag{3.28}$$

If all the erodible particles are removed, the porosity of the medium will attain a maximum (limiting) value

$$\phi_{\max} = 1 - V_n \tag{3.29}$$

Eq. (3.28) thus becomes

$$V_e = \phi_{\max} - \phi \tag{3.30}$$

If V_e has N_e particles with mean diameter d we then have

$$V_e = N_e \frac{\pi d^3}{6}. \tag{3.31}$$

i.e.

$$N_e = \frac{6}{\pi d^3}(\phi_{\max} - \phi) \tag{3.32}$$

Let N_s be the number of suspended particles in the mixture (water + particles).

The volume concentration of suspended particles in the mixture is then

$$C = \frac{N_s \frac{\pi d^3}{6}}{V_v} = \frac{N_s \frac{\pi d^3}{6}}{\phi} \tag{3.33}$$

i.e.
$$N_s = \frac{6}{\pi d^3}\phi C \tag{3.34}$$

As flows in porous media are very slow, the drag force exerted by the fluid on fine particles may be assumed to be governed by the well-known formula derived by Stokes for drag on a sphere of diameter *d*. i.e.

$$F_D = \lambda^* \mu v d \tag{3.35}$$

where λ^* is a coefficient that takes into account the effects of neighbouring spheres [see Bear (1972)].

We may first assume that the rate of erosion due to viscous drag is proportional to the total drag force acting on N_e erodible particles, i.e.

$$S_D = aF_D N_e = a\lambda^* \mu v d \times \frac{6}{\pi d^3}(\phi_{\max} - \phi) = \frac{6a\lambda^* \mu}{\pi d^2}(\phi_{\max} - \phi)v \tag{3.36}$$

where a is an empirical constant.

Note that in the above equation, the number of erodible particles N_e has been replaced by Eq. (3.32).

In terms of the discharge $q = \phi v$, this equation becomes

$$S_D = \frac{6a\lambda^* \mu}{\pi d^2}(\phi_{\max} - \phi)\frac{q}{\phi} \tag{3.37}$$

According to Hughes (1954), the viscosity μ for a suspension of spherical particles may be determined by the Einstein equation

$$\mu = \mu_0 (1 + 2.5C) \tag{3.38}$$

where μ_0 is the initial viscosity of the fluid (i.e. water in the present case) .

For small concentrations ($C < 0.01$), we may neglect the effect of variable viscosity on the rate of erosion.

Subsequently, as they move through the pores, the eroded particles may collide with the fixed particles and dislodge them from the solid matrix. It is therefore reasonable to assume that the erosion rate is increased by the transfer of momentum of the N_s moving particles to the N_e fixed particles. In other words, the erosion rate due to particle-particle interactions should be an increasing function of the velocity of the moving particles and of the number of collisions between moving and fixed particles. Noting that the momentum of a sphere of mass $m = \rho_s \frac{\pi d^3}{6}$ and velocity v, is $M = mv = \rho_s \frac{\pi d^3}{6} v$, the erosion rate due to momentum transfer may be expressed as

$$S_M = b(MN_s)N_e = b\rho_s \frac{\pi d^3}{6} v \times \frac{6}{\pi d^3}\phi C \times \frac{6}{\pi d^3}(\phi_{\max} - \phi) = \frac{6b\rho_s}{\pi d^3}(\phi_{\max} - \phi)\phi C v$$

i.e.
$$S_M = \frac{6b\rho_s}{\pi d^3}(\phi_{\max} - \phi) C q \tag{3.39}$$

where b is also an empirical constant.

By combining the effects of viscous drag due to fluid-particle interactions and the momentum transfer due to particle-particle collisions, it is possible to obtain the following combined equation for the erosion rate:

$$\begin{aligned} S &= S_D + S_M \\ &= \frac{6a\lambda^* \mu}{\pi d^2}(\phi_{\max} - \phi)\frac{q}{\phi} + \frac{6b\rho_s}{\pi d^3}(\phi_{\max} - \phi) qC \\ &= \frac{6}{\pi d^2}\rho_s (\phi_{\max} - \phi) q \left[\frac{a\lambda^* \mu}{\rho_s \phi} + \frac{b}{d} C \right] \end{aligned} \tag{3.40}$$

which may be written in the more concise form

$$S = \rho_s (\phi_{\max} - \phi) q \left[\frac{A}{\phi} + BC \right] \tag{3.41}$$

with $$A = \frac{6a\lambda^* \mu}{\pi d^2 \rho_s} \tag{3.42}$$

$$B = \frac{6b}{\pi d^3} \tag{3.43}$$

where a, b and λ^* are constant parameters to be determined empirically. The first term in parenthesis represents the removal of particles due to the imposed wall shear stress while the second term represents the action of collisions or momentum transfer between the moving and bound particles to detach the latter.

3.5 The coupled system of equations governing the internal erosion process

In summary, we have shown that the problem of internal erosion and fluid flow across a porous medium may be determined by a coupled system of equations consisting of the Darcy equation for the fluid flow, the constitutive equation for the rate of erosion of fine particles, and the transport equation for eroded particles:

$$q = -(k/\mu)(dP/dx + \rho g dz/dx) \tag{3.44}$$

$$\frac{\partial \phi}{\partial t} = (\phi_{\max} - \phi) q \left[\frac{A}{\phi} + BC \right] \tag{3.45}$$

$$\frac{\partial (C\phi)}{\partial t} + q \frac{\partial C}{\partial x} = \frac{\partial \phi}{\partial t} \tag{3.46}$$

This system of equations is to be solved under the given initial and boundary conditions.

CHAPTER IV - NUMERICAL SOLUTIONS TO THE PROBLEM OF INTERNAL EROSION

In the previous chapter, we have shown that the internal erosion process is governed by the following system of equations:

$$q = -(k/\bar{\mu})(dP/dx + \rho g dz/dx) \tag{4.1}$$

$$\frac{\partial \phi}{\partial t} = (\phi_{\max} - \phi) q \left[\frac{A}{\phi} + BC \right] \tag{4.2}$$

$$\frac{\partial (C\phi)}{\partial t} + q \frac{\partial C}{\partial x} = \frac{\partial \phi}{\partial t} \tag{4.3}$$

With k to be determined by the following equations

$$\mu = \mu_0 (1 + 2.5C) \tag{4.4}$$

$$k = k_0 \frac{\phi^3}{\left[(1-\phi) + \frac{\sqrt{2k_o}}{R_o} \right]^2} \tag{4.5}$$

In this chapter, we will present the solutions to these equations with the following initial and boundary conditions imposed:

1. Initial conditions

At $t = 0$ we have $C = C_0$, $\phi = \phi_0$

2. Boundary conditions

At x = 0, we have $P = P_0$, $C = C_0$

which corresponds to an inflow with a fixed concentration.

At $x = L$, we have $P = P_L$

Method of solution

The coupled system for q, ϕ and C may be solved by the explicit finite-differences method according to the following flow chart.

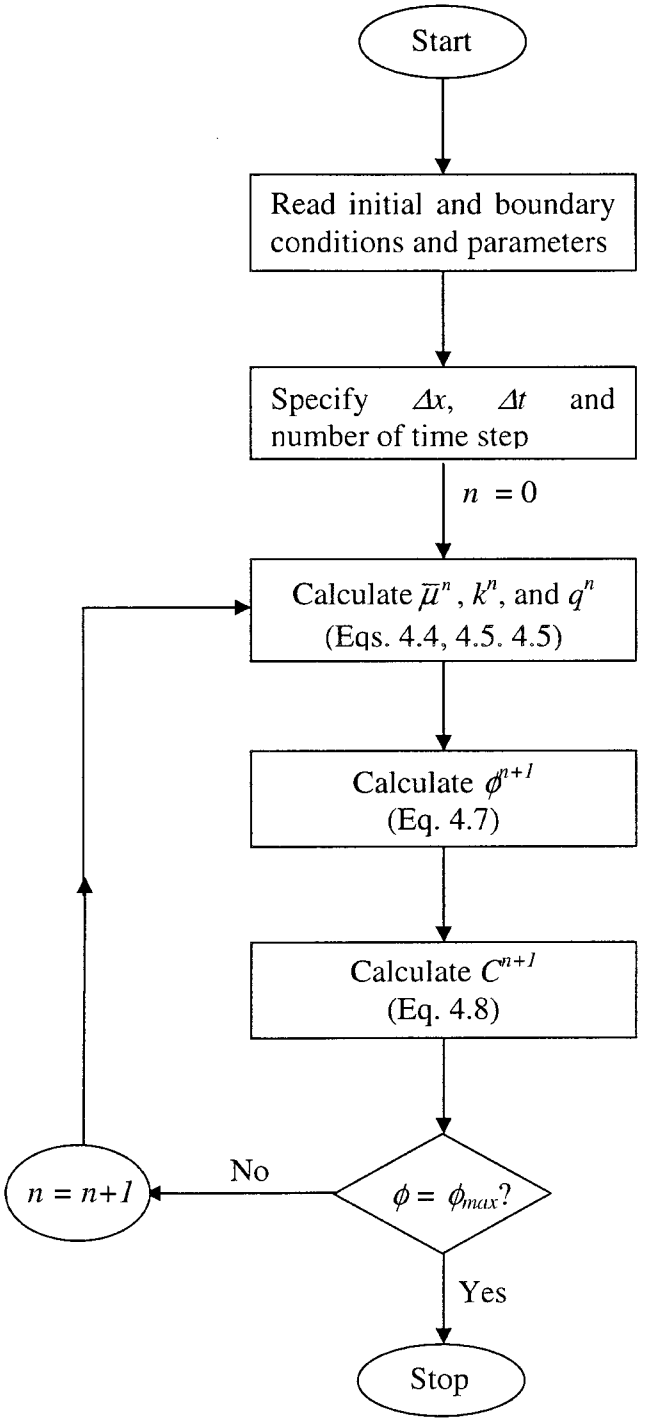

Figure 4.1: Flow chart of solution

Note in particular that, for a given k, the discharge q (which should be independent of x in the case of 1D flow) may be determined by a simple integration of the Darcy equation to obtain

$$q = -\frac{p_L - p_0}{\int_0^L \frac{\bar{\mu}}{k} dx} \tag{4.6}$$

The equations for the erosion rate and the transport of eroded particles have been solved numerically using a simple explicit finite difference scheme. A forward finite difference approximation is used to approximate the time derivative and a backward finite difference is used to approximate the spatial derivative, giving:

$$\frac{\phi_i^{n+1} - \phi_i^n}{\Delta t} = \left(\frac{\phi_{\max}}{\phi_i^n} - 1 \right) \left(A + B \phi_i^n C_i^n \right) q^n$$

$$\rightarrow \qquad \phi_i^{n+1} = \phi_i^n + \left(\frac{\phi_{\max}}{\phi_i^n} - 1 \right) \left(A + B \phi_i^n C_i^n q^n \right) \Delta t \tag{4.7}$$

$$\frac{c_i^{n+1}\phi_i^{n+1} - c_i^n \phi_i^n}{\Delta t} + q^n \frac{c_i^n - c_{i-1}^n}{\Delta x} = \frac{\phi_i^{n+1} - \phi_i^n}{\Delta t}$$

$$\rightarrow \qquad c_i^{n+1} = \frac{1}{\phi_i^{n+1}} \left[c_i^n \phi_i^n - \frac{\Delta t}{\Delta x} q^n \left(c_i^n - c_{i-1}^n \right) + \phi_i^{n+1} - \phi_i^n \right] \tag{4.8}$$

Once ϕ and C are calculated, the values of $\bar{\mu}$ and k are updated using equations (4.4) and (4.5) before computing q according to eq. (4.6).

The numerical solutions presented below have been obtained for the suffusion process, the backward erosion process and the mixed suffusion-backward erosion process, respectively.

The physical parameters used in the simulations are: L = 1 m, $\Delta P = P_L - P_0$ = 5000 Pa, $\phi_0 = 0.25$, $k_0 = 4\times10^{-11}$ m^2, $\rho_w = 998.2$ kg/m^3, $\rho_s = 2640$ kg/m^3, $\mu_0 = 1.002\times10^{-3}$ Ns/m^2.

Note that the chosen pressure difference ΔP corresponds to a hydraulic gradient i = 0.5 m/m , which is of the order of the critical gradient given in Table 1.3.

The permeabilty chosen here is an intermediate value in the wide range from 10^{-7} m^2 for well-sorted gravel to 10^{-15} m^2 for clay (see, e.g. Bear 1972).

Case 1: The suffusion process

If $B = 0$, which implies physically that no fixed particles are dislodged by collision and momentum transfer from moving particles, the erosion rate equation (4.2) becomes:

$$\frac{\partial \phi}{\partial t} = (\phi_{\max} - \phi) q \frac{A}{\phi}$$

which is exactly the model equation proposed by Bendahmane, with the parameter A designated as λ in his equation. It should be noted that the erosion coefficient A may have a very wide range of values. Bedahmane noted that A may vary from 0.0001 to 1. The results corresponding to the case A = 0.0001 have been presented in Bendahmane (2005). We therefore obtained the same results as those shown in figures 2.7 and 2.8, by choosing A = 0.0001 and the values of other parameters corresponding to his experiments.

We then considered the case of large values of A. For A = 1, $\phi_{max} = 0.4$, $C_0 = 0$, $\Delta t = 0.5$s, $\Delta x = 0.01$m, we obtain the following results:

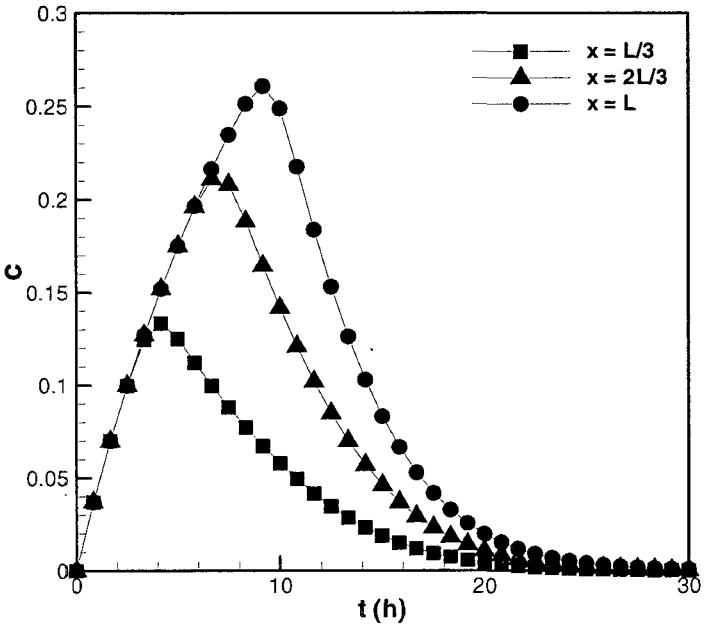

Figure 4.2: Time evolution of concentration

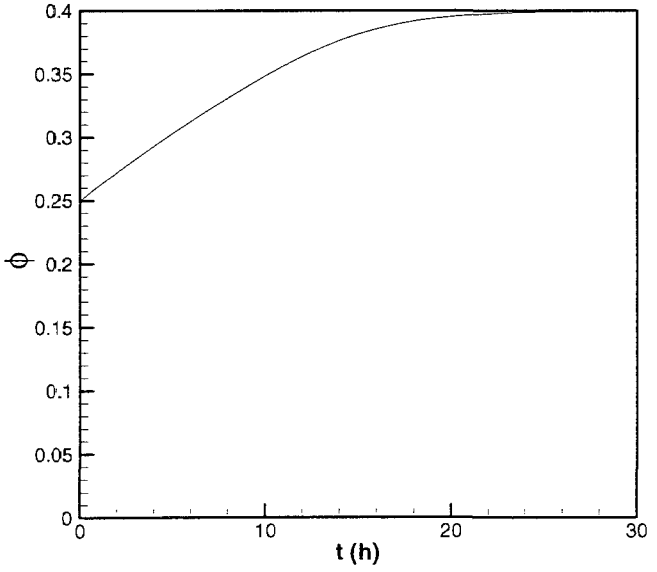

Figure 4.3: Time evolution of porosity

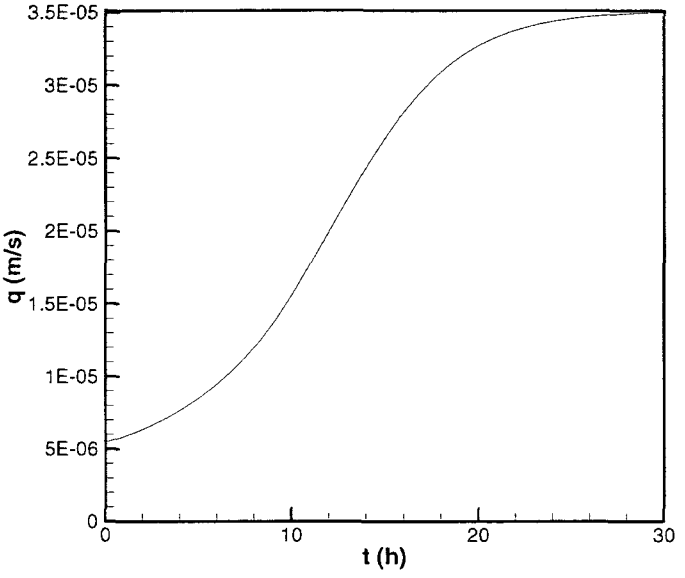

Figure 4.4: Time evolution of velocity

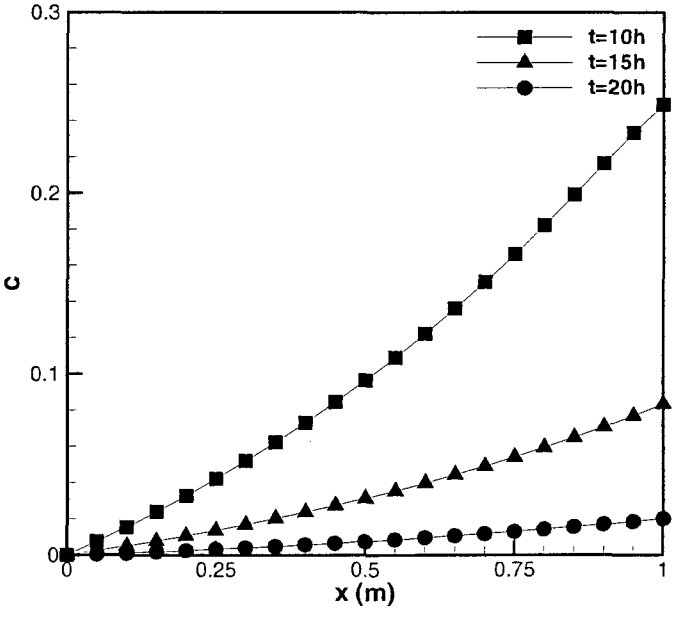

Figure 4.5: Spatial profiles of concentration at t = 10h, 15h and 20h

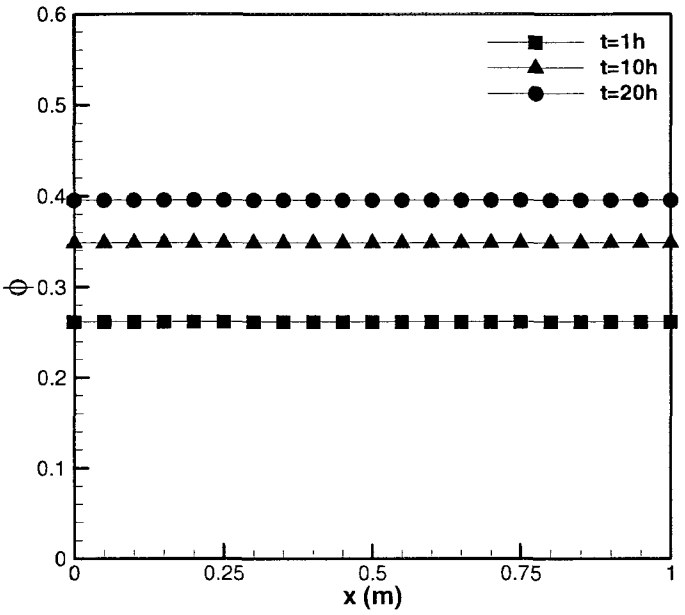

Figure 4.6: Spatial profiles of porosity at t = 10h, 15h and 20h

Figure 4.1 shows that the concentration C at each point increases at the beginning of the erosion process to attain a maximum value before decreasing asymptotically to 0. This may be expected as the result of two opposing effects, i.e. the accumulation of eroded particles being transported in the downstream direction and the decreasing erosion rate S with the passage of time. This is in agreement with the experimental results of Bendahmane (2005).

Figures 4.2, 4.3 and 4.5 indicate that both the porosity and average velocity increase with time, but do not change in space. This is a consequence of the flow being one-dimensional and the erosion rate being independent of the particle concentration which was found to increase spatially in the downstream direction while decreasing overall at later times as may be seen from Figure 4.4.

Figures 4.6 to 4.8 indicate the influence of the parameter A on the solutions. In this series of computations, A was varied from 0.5 to 2. Since A may be interpreted as a coefficient representing the facility with which the fine particles may be removed, the evolutions of concentration, porosity and discharge velocity occur at an increased rate for higher values of A as illustrated by Figures 4.6 - 4.8.

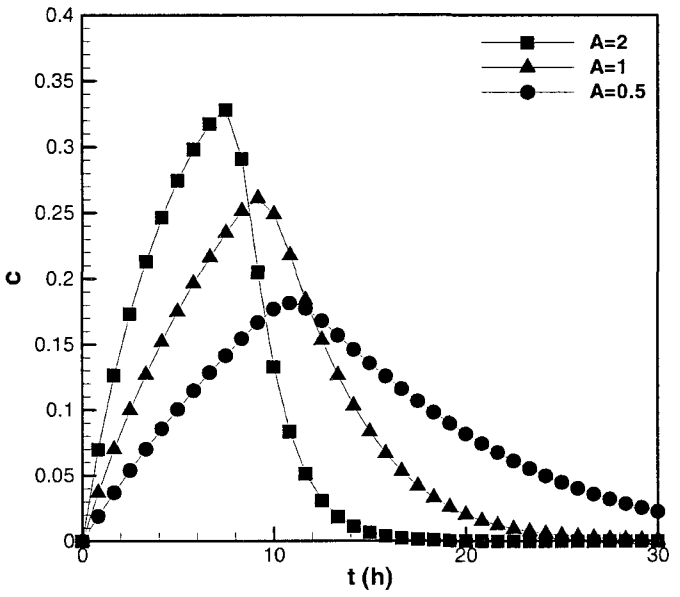

Figure 4.7: Time evolution of concentration at $x = L$ with different values of A

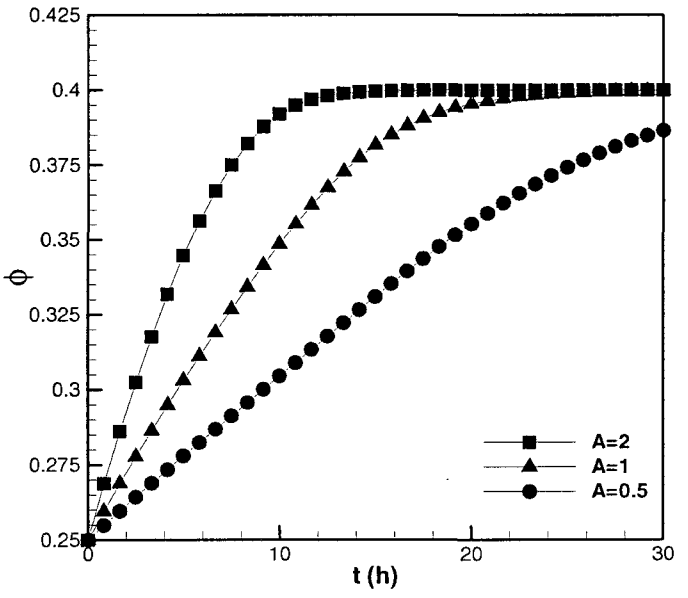

Figure 4.8: Time evolution of porosity with different values of A

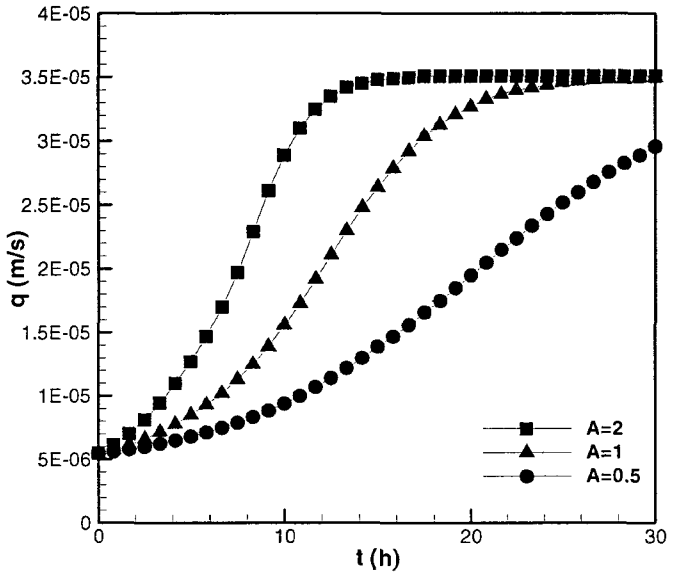

Figure 4.9: Time evolution of velocity with different values of A

Case 2: The Backward erosion process

With $A = 0$, the erosion rate equation simplifies to:

$$\frac{\partial \phi}{\partial t} = (\phi_{\max} - \phi) qBC$$

which is exactly the model equation proposed by Vardoulakis et al. (1996), with our parameter B designated as λ in his equation. In this case it may be noted that erosion occurs purely due to collisions between the moving and stationary particles attached to the soil matrix. Also noteworthy is the fact that the process cannot be initiated if $C = 0$ since this implies pure water with no particles available for the collision mechanism.

In a study of the hydro-mechanical aspects of the sand production problem, Vardoulakis et al. (1996) considered that B may vary between 5 and 50, and have presented the results for the case $B = 10$.

Using the same set of parameters, we have first obtained, as expected, the same results as those of Vardoulakis et al. (1996) shown in Figures. 2.9 - 2.13.

Next, we have solved the problem for various values of B, e.g. B = 10, 15 and 20 in order to show the effects of this key parameter on the evolution of the backward process.

By choosing ϕ_{max} = 1, C_0 = 0.001 (a small non-zero value), Δt = 0.5s, Δx = 0.01m, the results obtained indicate that contrary to the previous case of pure suffusion, the porosity now increases in both time and space. This is clearly illustrated in figure 4.11. These results typically simulate the mechanism of backward erosion.

The results for B = 15, C_0 = 0.001 are shown in figures 4.10 - 4.14.

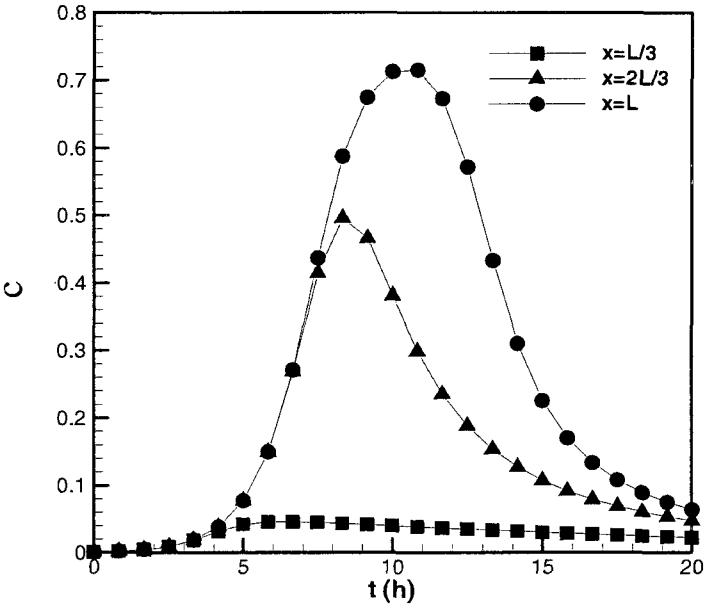

Figure 4.10: Time evolution of concentration

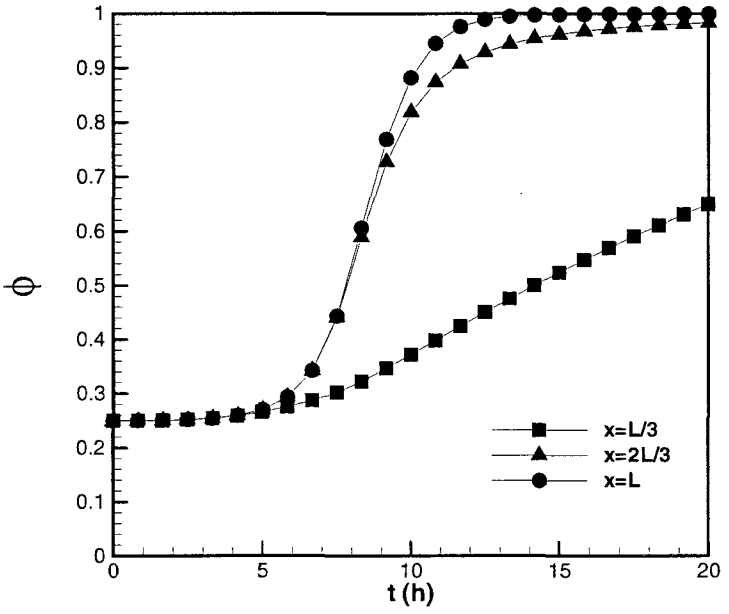

Figure 4.11: Time evolution of porosity

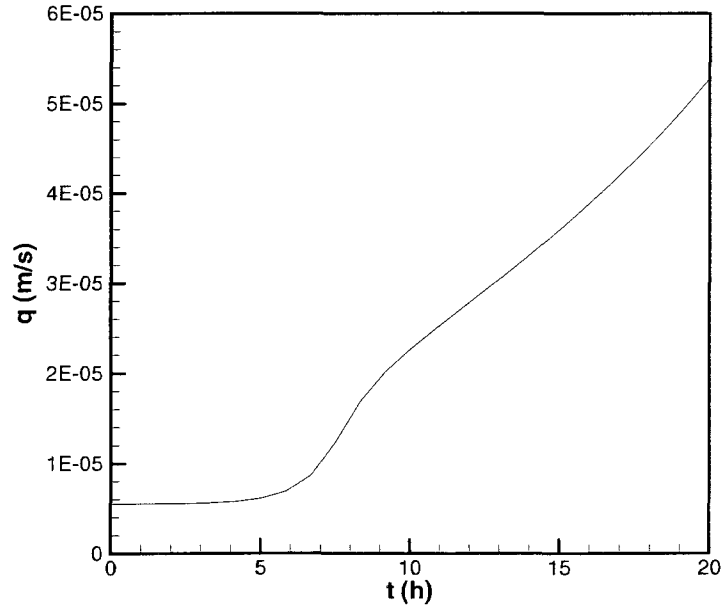

Figure 4.12: Time evolution of velocity

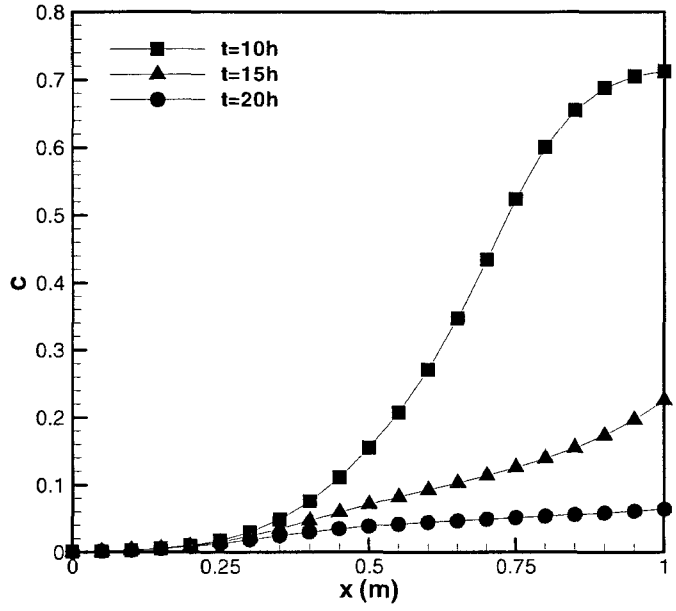

Figure 4.13: Spatial profiles of concentration at t = 10h, 15h and 20h

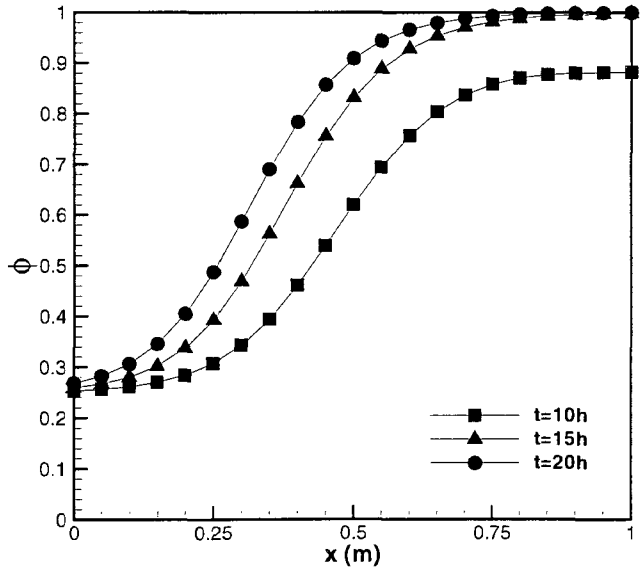

Figure 4.14: Spatial profiles of porosity at t = 10h, 15h and 20h

The following figures show the results obtained with B = 10, 15 and 20

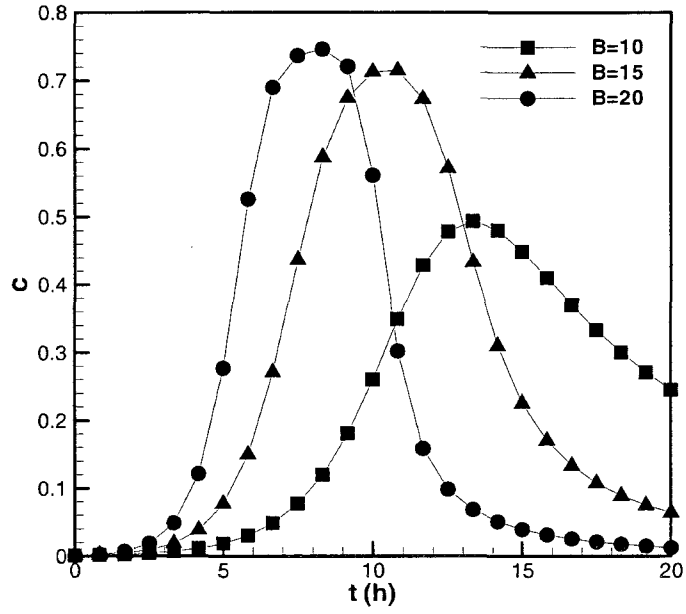

Figure 4.15: Time evolution of concentration at $x = L$ with different values of B

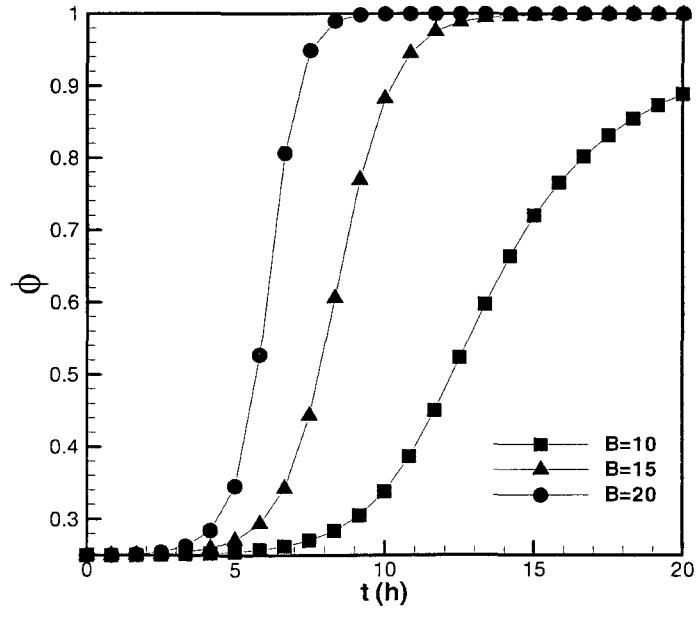

Figure 4.16: Time evolution of porosity at $x = L$ with different values of B

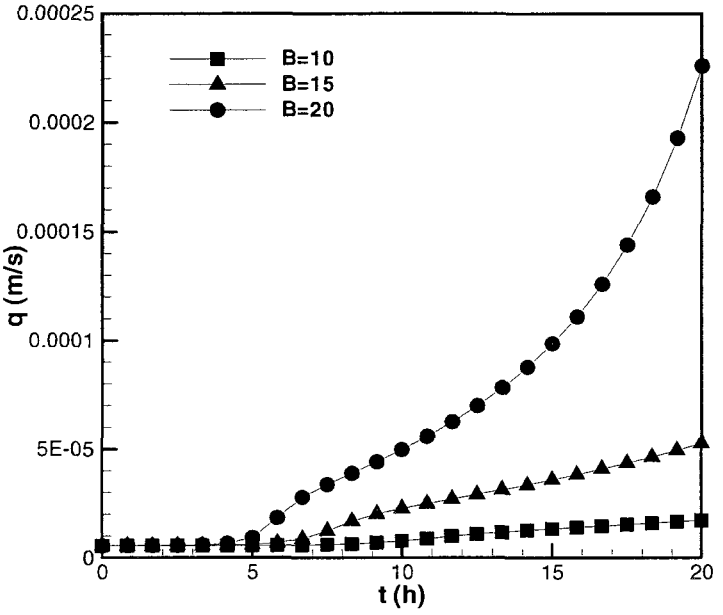

Figure 4.17: Time evolution of velocity with different values of B

In order to test the influence of the initial concentration C_0 on the final results, numerical experiments were run with $C_0 = 0.0005, 0.001, 0.0015$.

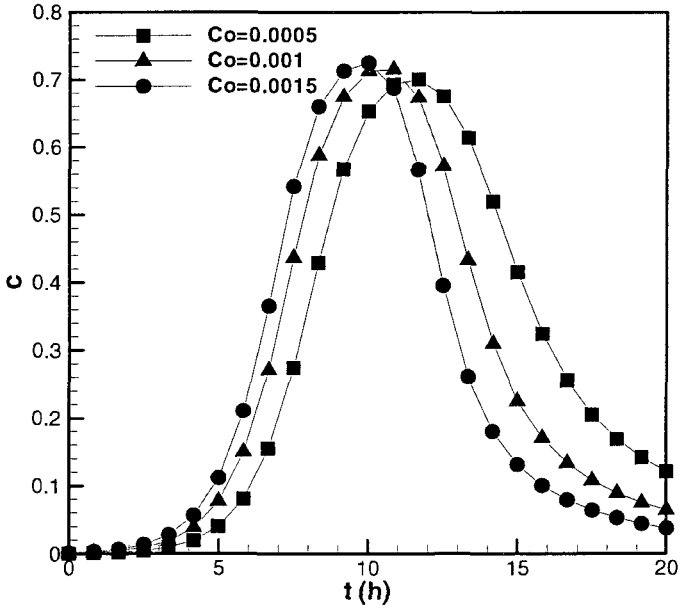

Figure 4.18: Time evolution of concentration at $x = L$ with different values of C_0

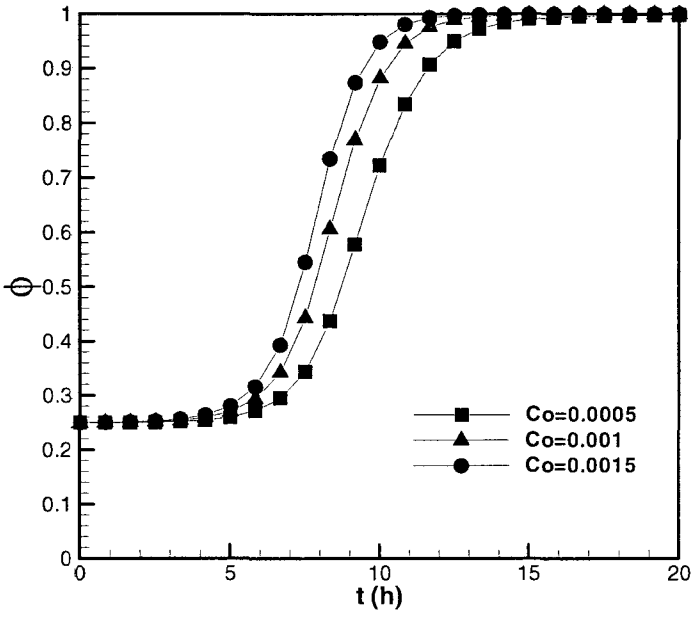

Figure 4.19: Time evolutions of porosity at $x = L$ with different values of C_0

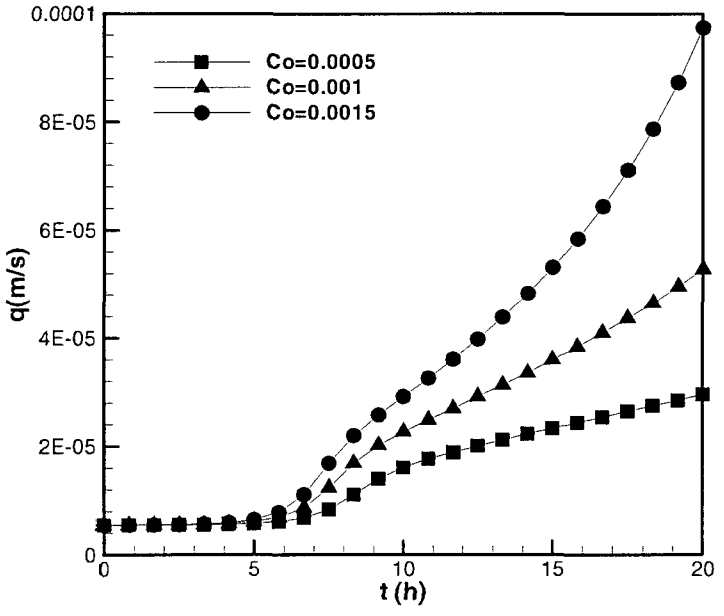

Figure 4.20: Time evolutions of velocity with different values of C_0

As expected, the results indicate that, except for some time shift in the values of porosity, concentration and velocity, the result of initially 'seeding' the flow (coefficient C_0) with particles does not appear to significantly affect the evolution of the process.

Case 3: The mixed process of suffusion and backward erosion

Let us now reconsider the previous case of backward erosion (with $A = 0$ and $B = 15$) in conjunction with a possible process of suffusion due to a non-zero value for A.

As mentioned above, the suffusion process is essentially determined by the erosion coefficient A which may have a wide range of values. We have therefore considered the effect of suffusion, with $A = 0.01$, 0.1 and 1, on the previous case of backward erosion (with $B = 15$). The results obtained are presented in the following figures which show that suffusion can very significantly accelerate the backward erosion process. In fact, a pipe is started by backward erosion (when $\phi = 1$ at $x = L$) after about 10h, 5h and 1.5h with $A = 0.01$, 0.1 and 1, respectively. This acceleration is due to the fact that the backward erosion rate is directly proportional to the concentration C of the eroded particle (eq. 3.39) which is greatly enhanced at earlier times (see Figure 4.2) under the effect of suffusion.

The results for $B = 15$ and $C_0 = 0$, and $A = 0.01, 0.1, 1$ are shown in Figures 4.21 to 4.23 respectively.

This series of results typically illustrate the combined mechanism of suffusion and particle-particle interaction that is supposed to occur in the internal erosion process in embankment dams.

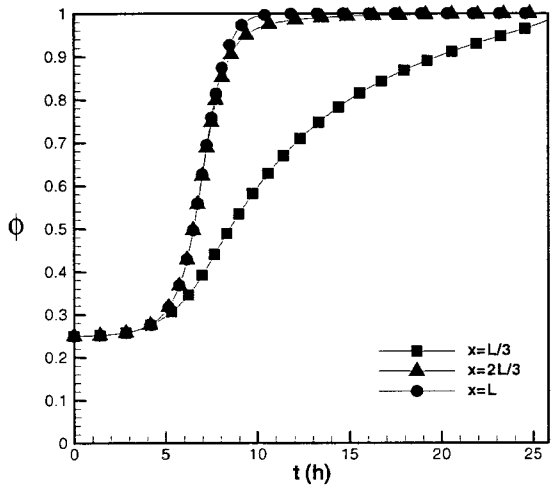

Figure 4.21: Time evolution of porosity with $A = 0.01$, $B = 15$

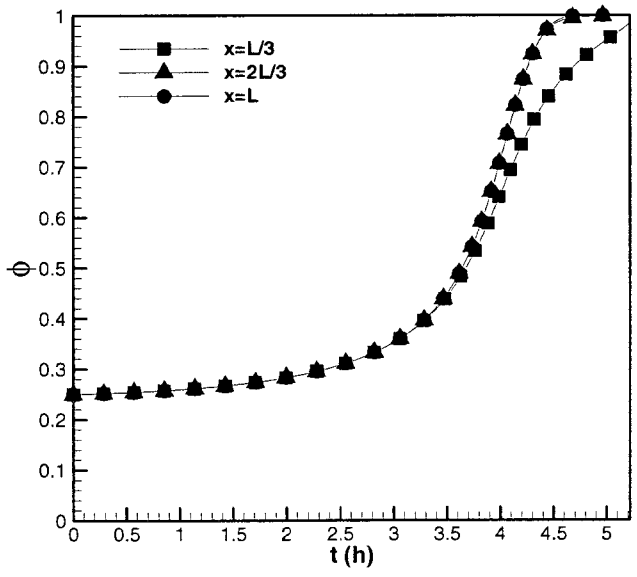

Figure 4.22: Time evolution of porosity with $A = 0.1$, $B = 15$

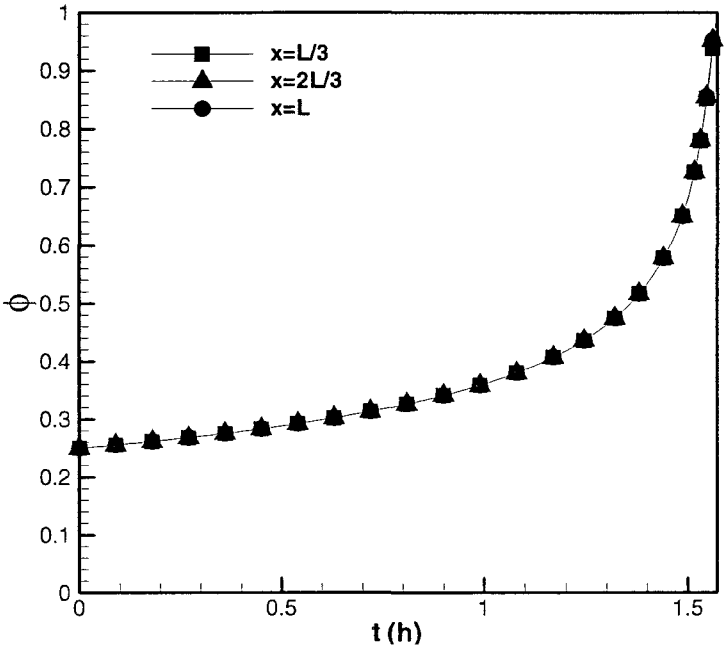

Figure 4.23: Time evolution of porosity with $A = 1, B = 15$

Case 4: Evolution of erosion to breach

To complete the description of internal erosion we now present some results of the evolution towards the breach stage. In fact, it has been observed that once the backward erosion stage has been completed, an 'empty' pipe within the embankment dam may have formed as illustrated in the figure below.

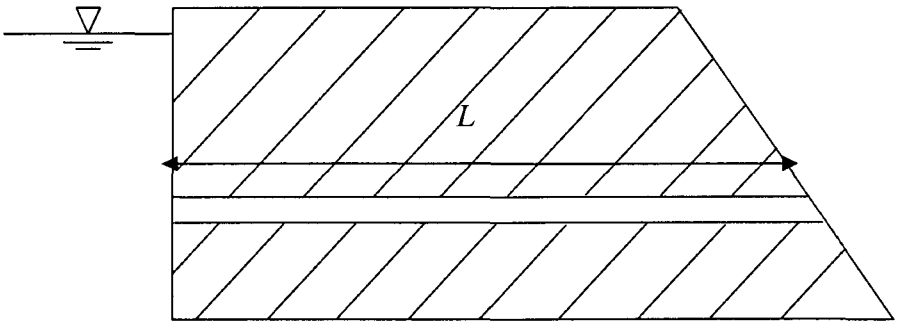

Figure 4.24: A schematic diagram of piping

We suppose a length L, an initial radius R_0 for this incipient pipe, and a pressure drop of ΔP between the upstream reservoir and downstream outlet. Based on the law of erosion by Fell et al. (2004), and by Bonelli et al. (2007), we suggest a new law of the form

$$r_{er} = k_{er}\tau_c\left(\frac{\tau}{\tau_c}-1\right)^n$$

where S is the rate of erosion per unit surface area of the pipe [kg/s/m^2], k_{er} is the coefficient of soil erosion [s/m], τ is the shear stress along the pipe [N/m^2], τ_c is the critical shear stress [N/m^2], and n is a correlative coefficient.

The wall shear stress along the pipe may be calculated by the following formula:

$$\tau = \frac{R\Delta P}{2L}$$

where R: radius of the pipe [m], ΔP: pressure drop [Pa], L: length of the pipe [m]

The relationship between the radius of the pipe and the rate of erosion may be expressed as

$$\frac{dR}{dt} = \frac{r_{er}}{\rho_s}$$

where R: radius of the pipe [m], S: rate of erosion [kg/s/m^2], ρ_s: density of the soil

The above equation may be discretized as

$$\frac{R^{n+1}-R^n}{\Delta t} = \frac{r_{er}}{\rho_s}$$

$$\rightarrow R^{n+1} = R^n + \frac{\Delta t \times r_{er}}{\rho_s}$$

For our problem at the breach stage we choose

C_e = 0.0005 s/m, τ_c = 20 Pa, ΔP = 5000 Pa, n = 1

Using the formula of Bonelli et al. (2007), the minimum radius for breach initiation may be estimated.

$$R_{\min} = \frac{2L\tau_c}{\Delta P} = \frac{2\times1\times20}{5000} = 0.008\,\text{m}$$

$$r_{er} = k_{er}\tau_c\left(\frac{\tau}{\tau_c}-1\right)^n = k_{er}\tau_c\left(\frac{\tau}{\tau_c}-1\right)$$

Let us assume that the maximum radius $R_{collapse}$ of the pipe just before collapse is

$$R_{collapse} = \frac{2\Delta P}{3g\rho_w} = \frac{2\times5000}{3\times9.8\times998.2} = 0.34\text{ m}$$

The results obtained are presented in the following figure:

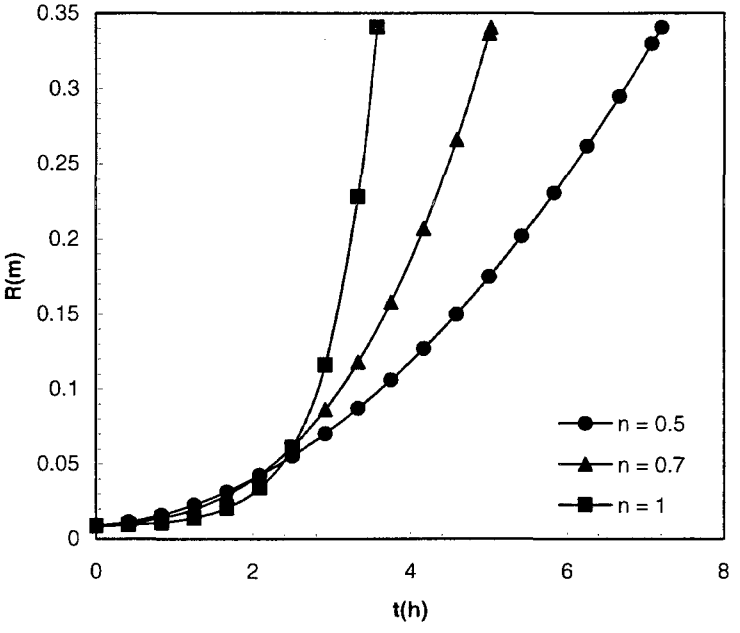

Figure 4.25: R vs t for various values of n

CHAPTER V - CONCLUSION

A study has been made of the internal erosion process in embankment dams and a model for the process has been constructed. The key to this problem is the constitutive equation relating the erosion rate S to the seepage flow through the dam. From a review of existing work on this problem, it was found that two typical equations have been found to correlate the experimental measurements: in the first one, Bendahmane (2005) by assuming that the erosion rate S should be a function of the porosity ϕ and the specific discharge q, obtained the equation $S = \rho_s \lambda \frac{1-\phi}{\phi} q$. From this equation, it was shown that the erosion rate as well as the porosity depends only on time, i.e. the erosion process is spatially uniform. This may represent the phenomenon of suffusion.

Another empirical equation has been obtained from the experiments of Vardoulakis (1996) who observed that the erosion rate depends not only on the porosity ϕ and specific discharge q, but also on the concentration C of the eroded particles, such that $S = \rho_s \lambda (1-\phi) C q$. It follows from this equation that the porosity ϕ as well as the concentration C will increase continuously toward the exit of the flow. This may therefore describe the so-called backward erosion behaviour. The objective of our work was therefore focused on the derivation of a unified constitutive equation for the erosion rate that may give rise to both suffusion and back erosion during the internal erosion process.

In order to solve the problem from a physical approach, we have considered embankment dams as a simple porous medium whose solid matrix is made up of two different types of particles, the 'fines' and the coarse particles. Under an imposed pressure difference between the upstream and downstream faces of the dam, it is assumed that the seepage flow is governed by the well-known Darcy law. Erosion should then be initiated by viscous forces acting on the fine particles as the fluid flows around them. We thus deduced a 'viscous erosion rate'

$$S_D = \frac{6a\lambda\mu}{\pi d^2}(\phi_{\max} - \phi)\frac{q}{\phi} \tag{5.1}$$

where 'a' is a coefficient to be determined.

This may be referred to as the erosion rate due to fluid-particle interactions.

We next considered collisions between the eroded particles that are already in motion with the fluid. Collisions between these particles and those at rest on the soil matrix may result in the latter being dislodged due to the momentum transfer from the former. We may then deduce a 'collision induced erosion rate'

$$S_M = \frac{6b\rho_s}{\pi d^3}(\phi_{\max} - \phi)Cq \tag{5.2}$$

where 'b' is a coefficient to be determined.

This may then be referred to as the erosion rate due to particle-particle interactions.

By combining the effects of both fluid-particle and particle-particle interactions, we propose that the process of internal erosion may be governed by the system of equations:

$$q = -(k/\bar{\mu})(dP/dx + \rho g dz/dx) \tag{5.3}$$

$$\frac{\partial\phi}{\partial t} = (\phi_{\max} - \phi)q\left[\frac{A}{\phi} + BC\right] \tag{5.4}$$

$$\frac{\partial(C\phi)}{\partial t} + q\frac{\partial C}{\partial x} = \frac{\partial\phi}{\partial t} \tag{5.5}$$

with $\bar{\mu}$ and k being determined by

$$\bar{\mu} = \mu_w(1 + 2.5c) \tag{5.6}$$

$$k = k_0\frac{\phi^3}{\left[(1-\phi) + \frac{\sqrt{2k_o}}{R_o}\right]^2} \tag{5.7}$$

The numerical solutions obtained from this model show that the erosion process follows the well-known sequence of: suffusion → backward erosion → piping enlargement → breach. In the case where $A \rightarrow 0$, this model converges towards the model of Bendahmane (2005) while the model of Vardoulakis (1996) corresponds to the case $B \rightarrow 0$.

However, it should be noted that the proposed model is limited by many approximations. In fact, embankment dams are not composed of a simple homogeneous porous medium made up of spherical particles, and the water flow is not necessarily a one-dimensional Darcy flow. Clearly as the internal particles are removed, Darcy's law becomes increasingly inapplicable and a new expression that changes seamlessly from Darcy flow to fully developed pipe flow as porosity increases is required. Furthermore, internal erosion and the causes of dam failures are not limited to the action of hydrodynamic forces.

This model should therefore be considered as a starting point for further study. In light of the results obtained in this work, it is reasonable to expect that a better erosion law may be of the form

$$S = (q - q_o)^m \left[\alpha + \beta (C - C_0)^n\right] \tag{5.8}$$

where α, β, m, n, q_0 and C_0 are constants to be determined. These constants are dependent on the soil structure as well as the intensity of the seepage velocity, and should be rather difficult to determine.

REFERENCES

Bear, J. (1972). *Dynamics of fluids in porous media.* New York: American Elsevier Publication Company.

Bendahmane, F. (2005). *Influence des interactions mécaniques eau-sol sur l'érosion interne.* Ph.D., École doctorale mécanique, thermique et génie civil, Nantes, France.

Bonelli, S., Marot, D., Ternat, F. & Benahmed, N. (2007). Criteria of erosion for cohesive soils. *7th ICOLD European dam symposium.* Freising, German: ICOLD.

Bonelli, S., Olivier, B., & Damien L. (2007). The scaling law of piping erosion. *18ème Congrès français de mécanique.* Grenoble, France: AFM, Maison de la Mécanique.

Cividini, A., & Gioda, G. (2004). Finite-element approach to the erosion and transport of fine particles in granular soils. *International journal of geomechanics, 4*(3), 191-198.

Fell, R. (2005). *Geotechnical engineering of dams.* Leiden, (The Netherlands): A.A. Balkema Publishers.

Fell, R., & Fry, J. (2007). *Internal erosion of dams and their foundations: selected and reviewed papers from the Workshop on Internal Erosion and Piping of Dams and their Foundations, Aussois, France, 25-27 April, 2005.* London: Taylor & Francis.

Fry, J.J. (2007). Context and framework of the report of the European working group on internal erosion. *7th ICOLD European dam symposium.* Freising, German: ICOLD.

Golzé, A.R. (1977). *Handbook of dam engineering.* The United States of America: Van Nostrand Reinhold Company.

Hughes, A.J. (1954). The Einstein relation between relative viscosity and volume concentration of suspensions of spheres. *Nature, 173,* 1089-1090.

Khilar, K.C., & Fogler, H.S. (1998). *Migration of fines in porous media.* The Netherlands: Kluwer Academic Publishers.

Liu, H. (2003). *Pipeline engineering.* The United States of America: CRC Press LLC.

Papamichos, E., Vardoulakis, I., Tronvoll, J. & Skjærstein, A. (2001). Volumetric and sand production model and experiment. *International journal for numerical and analytical methods in geomechanics, 25*, 789-808.

Papamichos, E., & Vardoulakis, I (2005). Sand erosion with a porosity diffusion law. *Computers and geotechnics, 32*, 47-58.

Perzlmaier, S., Muckenthaler, P. & Koelewijin, A. (2007). Hydraulic criteria for internal erosion in cohesionless soil. *7th ICOLD European dam symposium.* Freising, German: ICOLD.

Sterpi, D. (2003). Effects of the erosion and transport of fine particles due to seepage flow. *International journal of geomechanics, 3*(1), 111-121.

Terzaghi, K. (1967). *Soil mechanics in engineering practice.* New York: Wiley.

Vardoulakis, I., Stavropoulou, M., & Papanastasiou, P. (1996). Hydro-mechanical aspects of the sand production problem. *Transport in porous media, 22*, 225-244.

Vardoulakis, I. (2006). Sand production: mathematical modeling. *European journal of environmental and civil engineering, 10*(6-7), 817-828.

Wan, C.W., Fell, R., Cyganiewicz, J. & Foster, M. (2003). Time for development of internal erosion and piping in embankment dams. *Journal of geotechnical and geoenvironmental engineering, 119*(4), 307-314.

Wan, C.W., & Fell, R. (2004). Investigation of rate of erosion of soils in embankment dams. *Journal of geotechnical and geoenvironmental engineering, 130*(4), 373-380.

APPENDIX A

DERIVATION OF DARCY EQUATION

1. The capillary tube model

This is one of the simplest models where the porous medium is represented as a bundle of cylindrical tubes. The figure below shows a porous element of volume V, with a unit square section, containing N capillary tubes of radius R and length L. The rest is solid.

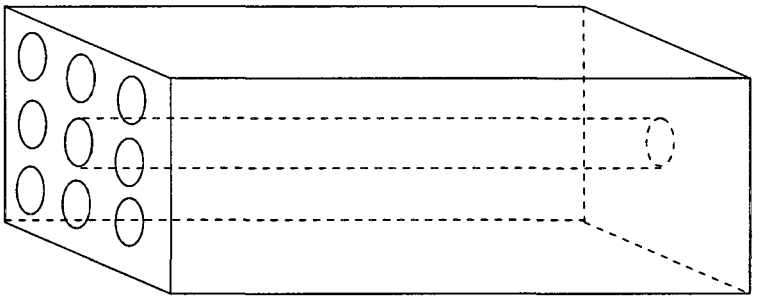

Figure A.1: Schematic structure of a porous medium

The porosity of this medium is

$$\phi = \frac{V_v}{V} = \frac{N\pi R^2 L}{1\times 1\times L} = N\pi R^2 \tag{A.1}$$

Note that the 'surface' porosity is also

$$\phi = \frac{A_v}{A} = \frac{N\pi R^2}{1\times 1} = N\pi R^2 \tag{A.2}$$

where

V_v: the total volume of N tubes

V: the volume of the porous element

A_v: the total area of pores (voids) in a cross-section

A: the area of the cross-section

Let us now consider an elementary cylinder of radius r and length Δx within a tube as shown below

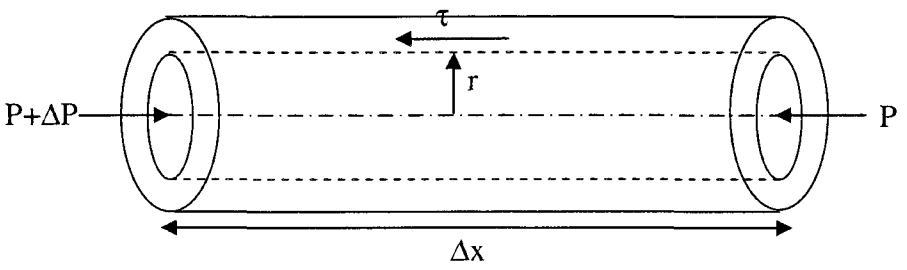

Figure A.2: Elementary cylinder

The forces acting on this element are the pressure force, shear force, and gravity force. The balance of forces for this elementary cylinder (considered horizontal, for simplicity) is

$$\sum F = 0 \tag{A.3}$$

i.e. $$\Delta P \pi r^2 = \tau \times 2\pi r \Delta x \tag{A.4}$$

therefore $$\tau = \frac{r\Delta P}{2\Delta x} \tag{A.5}$$

Now according to Newton's law for the shear force τ, we have

$$\tau = -\mu \frac{dv}{dr} \tag{A.6}$$

We thus deduce

$$\frac{r\Delta P}{2\Delta x} = -\mu \frac{dv}{dr} \tag{A.7}$$

i.e. $$\frac{dv}{dr} = -r \frac{\Delta P}{2\mu \Delta x} \tag{A.8}$$

from which we integrate to obtain

$$v = -\left(r^2 + const\right) \frac{\Delta P}{4\mu \Delta x} \tag{A.9}$$

By applying the boundary condition $v = 0$ at $r = R$, we get the well-known parabolic velocity distribution:

$$v = \left(R^2 - r^2\right)\frac{\Delta P}{4\mu\Delta x} \tag{A.10}$$

The mean velocity in the tube is then given by

$$\overline{v} = \frac{1}{A}\int_0^R v dA = \frac{1}{\pi R^2}\int_0^R \left(R^2 - r^2\right)\frac{\Delta P}{4\mu\Delta x} \times 2\pi r dr = \frac{\Delta P R^2}{8\mu\Delta x} \tag{A.11}$$

In terms of the average velocity or discharge q, we have $\overline{v} = \frac{q}{\phi}$. We may therefore write the above equation as

$$q = \frac{\phi R^2}{8\mu}\frac{\Delta P}{\Delta x} \tag{A.12}$$

or, putting $k = \phi R^2/8$, we have

$$q = -\frac{k}{\mu}\frac{dP}{dx} \tag{A.13}$$

which shows that this model leads to the Darcy law with a permeability given by

$$k = \phi R^2/8. \tag{A.14}$$

2. The flow resistance model

It is well known that as a fluid is moving along the surface of a solid body, it exerts a force on that surface. This force has two components: The shear stress, tangential to the boundary which is due to the viscosity and velocity gradient; and the pressure force, normal to the surface, which is due to the variation of pressure along the surface. The sum of these two forces along the entire surface of the considered body gives the resultant force. The component of this force in the direction of the velocity v is called the drag (force) F_D. The component normal to the velocity is called the *lift*. The drag is usually expressed in the form

$$F_D = C_D\frac{\rho v^2}{2}A \tag{A.15}$$

where A is the frontal area normal to v and C_D is the non-dimensional drag coefficient.

For simplicity, we may use the Stokes drag on a sphere of diameter d as an analogy to the drag on the particles of a porous medium:

$$F_D = 3\pi d\mu v \tag{A.16}$$

If we have N such spheres in a elementary volume (EV) of porous medium that has the form of a cylinder of length ds in the direction of flow and a cross section dA, then

$$N = 6(1-\phi)dAds / \pi d^3 \tag{A.17}$$

Summing the forces acting on the EV leads to

$$p\phi dA - (p + \frac{\partial p}{\partial s} ds)\phi dA - (\rho g \phi dAds)\frac{\partial z}{\partial s} - NF_D = 0 \tag{A.18}$$

$$-\frac{\partial h}{\partial s} - \frac{NF_D}{\rho g \phi dAds} = 0, \quad where \quad h = z + p/\rho g \tag{A.19}$$

Replacing the formula for N and F_D in this equation, we obtain

$$-\frac{\partial h}{\partial s} = \frac{6\lambda(1-\phi)\mu}{\pi d^2 \phi \rho g} v \tag{A.20}$$

$$q = -\frac{\pi\phi^2}{6\lambda(1-\phi)} d^2 \frac{\rho g}{\mu} \frac{\partial h}{\partial s} \tag{A.21}$$

which may be written as

$$q = -(k\frac{\rho g}{\mu})\frac{\partial h}{\partial s} \tag{A.22}$$

with

$$k = \pi\phi^2 / 6\lambda(1-\phi)d^2 \tag{A.23}$$

which represents the permeability in the one-dimensional Darcy equation.